INFORMATION TO USERS

This manuscript has been reproduced from the microfilm master. UMI films the text directly from the original or copy submitted. Thus, some thesis and dissertation copies are in typewriter face, while others may be from any type of computer printer.

The quality of this reproduction is dependent upon the quality of the copy submitted. Broken or indistinct print, colored or poor quality illustrations and photographs, print bleedthrough, substandard margins, and improper alignment can adversely affect reproduction.

In the unlikely event that the author did not send UMI a complete manuscript and there are missing pages, these will be noted. Also, if unauthorized copyright material had to be removed, a note will indicate the deletion.

Oversize materials (e.g., maps, drawings, charts) are reproduced by sectioning the original, beginning at the upper left-hand corner and continuing from left to right in equal sections with small overlaps. Each original is also photographed in one exposure and is included in reduced form at the back of the book.

Photographs included in the original manuscript have been reproduced xerographically in this copy. Higher quality 6" x 9" black and white photographic prints are available for any photographs or illustrations appearing in this copy for an additional charge. Contact UMI directly to order.

UMI®

Bell & Howell Information and Learning
300 North Zeeb Road, Ann Arbor, MI 48106-1346 USA
800-521-0600

Negative Skin Friction on Single Piles in Clay Subjected to Direct and Indirect Loading

Ali Sharif

A Thesis
in
The School For Building
(Civil Engineering Program)

Presented in Partial Fulfillment of the requirements
for the Degree of Master of Applied Science at
Concordia University
Montreal, Quebec, Canada

March 1998

ABSTRACT

Negative Skin Friction on Single Piles in Clay Subjected to Direct and Indirect Loading

Ali Sharif

A numerical model employing the finite element technique is developed to analyze the negative skin friction induced in single floating piles subjected to direct and indirect loading. The pile is embedded in saturated clay. The clay is subjected to surcharge pressure for generating indirect loading on the pile. The soil is assumed to behave as a linearly elastic perfectly plastic material with a yield function defined by the Mohr-Coulomb equation. The results of the numerical model compared well with the field data. A parametric study is presented to show the influence of various parameters on the location of neutral plane. It has been found that the level of direct loading introduced in terms of factor of safety has a major effect in locating the neutral plane. Based on the results of the present investigation, a design formula together with design charts are given for determining the allowable bearing capacity of coated and uncoated single piles.

ACKNOWLEDGEMENTS

I would like to express my sincere gratitude to my supervisor, Professor **A. M. Hanna**, for his valuable guidance, constant support and encouragement throughout the course of this investigation.

The financial support from The Libyan Ministry of Education is highly appreciated.

I wish also to thank my family, my parents, and my wife and children for their support and encouragement during the preparation of this work.

TABLE OF CONTENTS

LIST OF FIGURES

LIST OF TABLES

LIST OF SYMBOLS

SYMBOL	REPRESENTS
A	Area.
a	Soil attraction.
A_s	Area of the pile shaft.
A_t	Cross-sectional area of the pile tip.
B	Height of finite element mesh.
C	Circumference of the pile.
c	Soil cohesion.
C_1, C_2	soil strength constants.
c_u	Undrained shear strength.
D	Pile diameter.
E_p	Pile modulus of elasticity.
E_s	Soil modulus of elasticity.
F_n	Downdrag load.
f_n	Factor of safety on the downdrag load.
F_n^m	Maximum downdrag load.
f_p	Factor of safety on the permanent load.
f_Q	Factor of safety on the ultimate bearing capacity.
f'_Q	Factor of safety on the ultimate shaft resistance.
FS	Factor of safety.
f_s	Factor of safety related to the allowable settlement.

f_t	Factor of safety on the transient load.
f(z)	Soil parameter similar to the inverse of modulus of elasticity that varies with depth.
G	Shear modulus of soil.
G_b	Shear modulus of soil at the pile tip.
g(z)	Soil parameter similar to the shear modulus that . varies with depth.
I_N	Downdrag influence factor.
k	Soil stiffness per unit pile length.
K_n	Slip element stiffness in normal direction.
K_o	Coefficient of earth pressure at rest.
K_{res}	Residual shear modulus of slip element.
K_s	Coefficient of earth pressure.
k_{si}	Initial tangent of the hyperbolic curve.
L	Length of the pile.
L_{NP}	Depth of neutral plane.
M	Friction factor for the soil acting on the pile surface.
m_v	Coefficient of volume decrease.
Ns	Surcharge pressure parameter.
N_t	Tip bearing capacity coefficient.
$\overline{P}$	Mean effective pressure.
P_a	Allowable bearing capacity.
P_b	Load carried by the pile tip.

P_h	Load applied on the pile head.
P_i	Nodal force.
P_l	The axial load .
P_m	Maximum load previously applied on the pile head.
P_p	Permanent load on the pile.
P_r	Residual load at the pile tip.
P_t	Transient load on the pile.
P_{ui}	Maximum nodal force.
P_{vz}	Reduced effective stress at depth z.
P_{vL}	Reduced effective stress at the pile tip.
P_z	Effective stress at depth z.
Q_d	Allowable dead load.
Q_{NP}	Total load at the neutral plane depth.
Q_s	Ultimate shaft resistance acting below the neutral plane.
Q_s^m	Ultimate shaft resistance acting along the full pile length.
Q_t	Ultimate tip resistance.
Q_u	Ultimate bearing capacity.
r_m	Maximum radius beyond which the deformation is ignored.
R_N	Reduction factor of downdrag load.
r_n	Roughness number.

r_o	Radius of the pile.
S	Surcharge pressure or surcharge loading.
S_n	Negative skin friction number.
S_o	Surface settlement of the soil.
S_t	Total relative settlement.
t	Thickness of slip element.
u_o	Excess pore pressure at the time of installation.
u_t	Excess pore pressure at time (t) after installation.
W	Width of finite element mesh.
w_b	Settlement of the pile tip.
w_i	Relative pile-soil settlement.
w_o	Local settlement of the pile.
w_p	Axial deformation of the pile.
w_{slip}	Required displacement to cause slippage at the pile-soil interface.
w_s	Vertical soil displacement.
γ	Shear strain.
γ'	Effective unit weight of soil.
γ_p	Unit weight of pile material.
λ	Negative skin friction coefficient.
β	Shaft resistance coefficient in effective stress method.
β_c	Shaft resistance coefficient in effective stress

	method in case of bitumen coating.
δ	Angle of shearing resistance in slip element.
δ_h	Settlement of the pile head.
δ_{sy}	Relative settlement required to yield the shaft resistance.
δ_{ty}	Relative displacement that yields the tip resistance.
τ_n	Negative skin friction.
$\overline{\tau_n}$	Average negative skin friction.
τ_n^m	Maximum negative skin friction.
τ_{nr}	Negative residual skin friction.
$\overline{\tau_p}$	Average positive skin friction.
τ_p^m	Maximum positive skin friction.
τ_{pr}	Positive residual skin friction.
μ	mobilized skin friction.
ν_p	Poisson's ratio of pile.
ν_s	Poisson's ratio of soil.
σ_1	Major effective principal stress.
σ_2	Intermediate effective principal stress.
σ_3	Minor effective principal stress.
σ'_v	Vertical effective stress.

CHAPTER 1
INTRODUCTION

1.1 PREFACE

The need for deep foundations has grown with the growth of civilization. Piled foundation, a subdivision of deep foundation, has been used and universally accepted as the traditional form of foundation in bad subsoil conditions. According to the manner they transmit loads to the resisting subsoil layers, piles can be classified into two broad categories, end-bearing and floating piles. An end-bearing pile usually rests on a relatively incompressible soil layer because of which the applied load is transmitted predominantly through the pile tip to the bearing layer. On the other hand, a floating pile is usually installed in a compressible soil layer beyond the reach of any incompressible bearing strata at its tip, thus it transmits the loads to the surrounding soil mainly through the pile shaft.

The bearing capacity determination of piles in normal soil conditions is based on the assumption that the pile penetrates downward while the surrounding soil remains in location to resist the pile movement. According to this assumption, the shaft resistance is induced by generating shear stresses, positive in sign, along the pile shaft, and the tip resistance is induced by generating normal stresses at the pile tip, as shown in Figure (1-1). In many circumstances settlement of the surrounding soil might take place, thus it will provide no support to the pile. As a matter of a fact, it will act in the reverse sense, in terms of resistance, by comparison with the normal situation. Further, if the downward movement of the surrounding soil exceeds the pile settlement, the pile will resist the soil

movement and hence an extra load will be transferred to it in addition to the external axial load. It has been found that the downdrag load due to surcharge loading (indirect loading) on the surrounding soil can exceed the ultimate capacity of a pile (Johanessen and Bjerrum, 1965). Moreover, the excessive settlement associated with the downdrag can cause vital damages to the superstructure of a building (Brand and Luangdilok, 1975). The shear stresses generated on the pile shaft by virtue of the soil settlement will be negative in sign, and accordingly the terms "negative skin friction" and "downdrag load" are used.

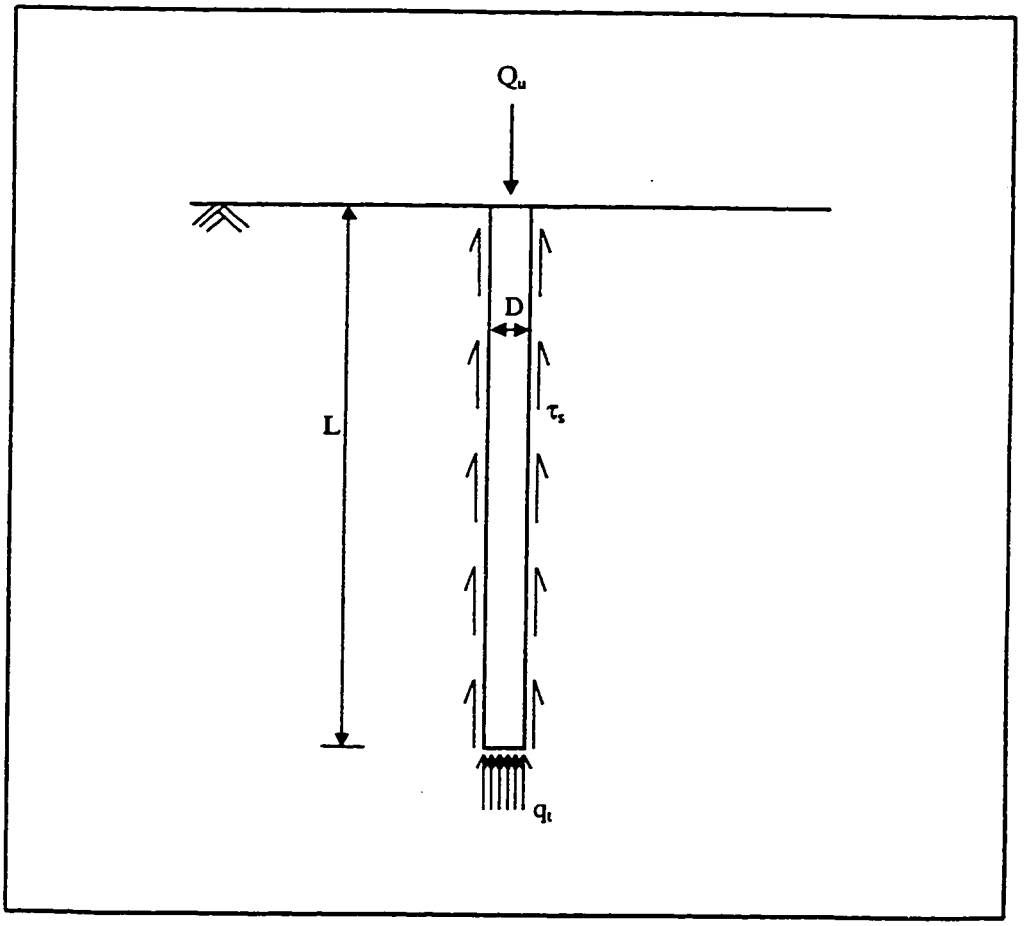

Figure (1-1) Axially loaded pile

The problem of negative skin friction is usually associated with normally consolidated or lightly overconsolidated deposites of clay. Therefore, the mode of settlement expected to cause negative skin friction will be normally of a long term one, which is known as the consolidation settlement . Consolidation of clay deposits may occur due to one or more of the following causes:

(a) under the soil own weight for recent filled deposites (Clement, 1984),

(b) direct loading on the soil surrounding the pile, such as, embankments and surcharge fills,

(c) direct loading on the soil adjacent to the pile, such as, shallow foundations of a new building and abutments of bridges (Bozozuk, 1970 and Garlanger, 1974),

(d) the fluctuation of groundwater table (Auvinet and Hanell, 1981), and

(e) the installation of driven piles in highly sensitive soils (Fellenius, 1972).

The negative skin friction is a function of the relative displacement between the pile and the surounding soil. Therefore, the negative skin friction distribution along the pile shaft of an end-bearing pile is different from that in the floating pile. For an end-bearing pile resting on a rigid stratum, the negative skin friction will be generated all over the entire shaft from the pile head to its tip. Whereas, for floating piles, the negative skin friction will be mobilized in the upper portion starting from the pile head to a neutral depth after which positive skin friction is mobilized in the lower portion. The neutral depth can also be defined as the depth at which the relative displacement between the pile and the ambient soil is zero.

1.2 RESEARCH OBJECTIVES

The objectives of this research program are as follows:

(a) to conduct a literature survey on negative skin friction focusing on the determination of the downdrag load and the location of the neutral plane,

(b) to develop a numerical model utilizing the finite element technique, for the case of a single pile embedded in clay and subjected to both axial and surcharge loading,

(c) to compare the resulting values obtained from the numerical model with those obtained from the existing theories and available field data,

(d) to conduct a parametric study on the effect of the pile size, the applied axial load on the pile, the surcharge loading on the surrounding soil, and the soil strength parameters on the location of the neutral plane, and

(e) to develop a design procedure and recomendations for future research for the determination of the location of the neutral depth.

1.3 THESIS OUTLINE

A literature review on negative skin friction is provided in chapter 2. In chapter 3, a description of the numerical model along with the types of loading applied in the study is presented. The results and discussion are given in chapter 4. Finally the conclusion and recommendations for future work on the subject are presented in chapter 5.

CHAPTER 2
LITERATURE REVIEW

2.1 GENERAL

Since the recognition of negative skin friction phenomenon in pile foundations, a considerable amount of research has been published on the subject. The majority of these publications were experimental work carried out either in the field and/or in the laboratory to investigate the negative skin friction induced by different causes on a single pile, such as, consolidation of highly sensitive soils due to pile installation (Fellenius, 1972), recent embankment fill (Bozozuk, 1972), or water table fluctuation (Auvinet and Hanell, 1981), and relating the developed downdrag load to either the initial overburden pressure or the initial undrained shear strength.

This chapter is therefore devoted to report the recent development of the determination of negative skin friction magnitude and area of application on piles in clay. These methods categorized under (a) semi-empirical methods, (b) computational procedures, (c) numerical techniques.

2.2 REVIEW OF PREVIOUS WORK

Zeevaert (1959) suggested a theoretical approach to evaluate the load capacity of end bearing piles subjected to negative skin friction. In his proposed theory, Zeevaert did not just take the imposed load due to downdrag into account , but he also included the reduction of the confining pressure at the bearing stratum which was attributed to the hang-up tendency of the settling soil.

The reduced effective stress was defined in terms of the initial effective stress by means of the limiting equilibrium equation which can be expressed, for a single pile, by the following equation:

$$P_{vz} = (\gamma'/m)\,(1 - e^{-mz}) + S\,e^{-mz} \qquad \ldots\ldots\ (2.1)$$

where P_{vz} = the reduced effective stress at depth z

γ' = the effective unit weight of soil

S = the surcharge pressure

$m = \pi D\beta$; $\beta = K_o \tan\phi$

The downdrag force acting on the pile shaft was represented by:

$$F_n = \int_0^L \pi D \beta P_{vz}\, dz \qquad \ldots\ldots\ (2.2)$$

integration of equation (2.2), after substituting for P_{vz}, will lead to:

$$F_n = (\gamma' L + S) - P_{vL} \qquad \ldots\ldots\ (2.3)$$

The assumption of the reduction in overburden pressure implicitly implies that the slippage between the pile and the soil will not occur. Thus, there is no compelling physical basis for this assumption.

Poorooshasb and Bozozuk (1967) introduced a closed form solution to an incompressible pile resting on bedrock, and embedded in a clay layer which acted upon by a surcharge loading and being permitted to drain from both upper and lower surfaces of the layer. It is further assumed that the presence of the pile has no effect on the dissipation of the pore water pressure.

The solution was based on an upper bound plastic analysis which utilizes a kinematically admissible displacement field that satisfies the overall equilibrium of the system. The displacement field considered was a product of two functions so the separation of variables is possible. In addition, the soil was modeled with constitutive equation that indicates an increase in stiffness with depth. Although rigorous, the solution is complex, involving infinite series and modified Bessel functions of the second kind, which makes it difficult to be utilized in practice.

Poulos and Mattes (1969) proposed an analytical method to predict the effects of negative skin friction on a single compressible pile of circular cross-section. The tip of the pile was assumed to rest on a perfectly rigid base, and the surrounding soil was assumed to be a homogeneous isotropic elastic material. By employing Mindlin equation for the vertical displacements of a point within a semi-infinite mass, solutions were obtained for the relationship between the surface settlement of the soil and the downdrag force induced in the pile. The influence, on this relationship, of relative stiffness of the pile, the length to diameter ratio, and Poisson's ratio of the soil was investigated.

The problem was solved by dividing the pile into equal cylindrical elements. Each element was acted upon by a uniform vertical shear stress on a mid point at the shaft. Furthermore, at each mid point, the displacement of the soil layer adjacent to the pile was equated to that of the pile itself. It is also assumed that the consolidation settlement of the soil remote from the pile varies linearly with depth from S_o at the surface to zero at the bottom, as shown in figure (2-1). A mirror-image technique was utilized in conjunction with Mindlin equation to enforce zero vertical displacement at the pile base, as to simulate

a rigid bearing stratum since Mindlin's solutions is strictly valid for a homogenous isotropic half-space. The expression presented to determine the maximum downdrag force is as follows:

$$F_n^m = I_N \cdot E_s \cdot S_o \cdot L \qquad \ldots\ldots (2.4)$$

where F_n^m = the maximum downdrag load

I_N = the downdrag influence factor

E_s = the elastic modulus of the soil

S_o = the surface settlement of the soil

L = the length of the pile

Slippage between the pile and the surrounding soil was considered in the approach by modifying the analysis to take into account for the local yielding at the pile-soil interface defined by Coulomb equation.

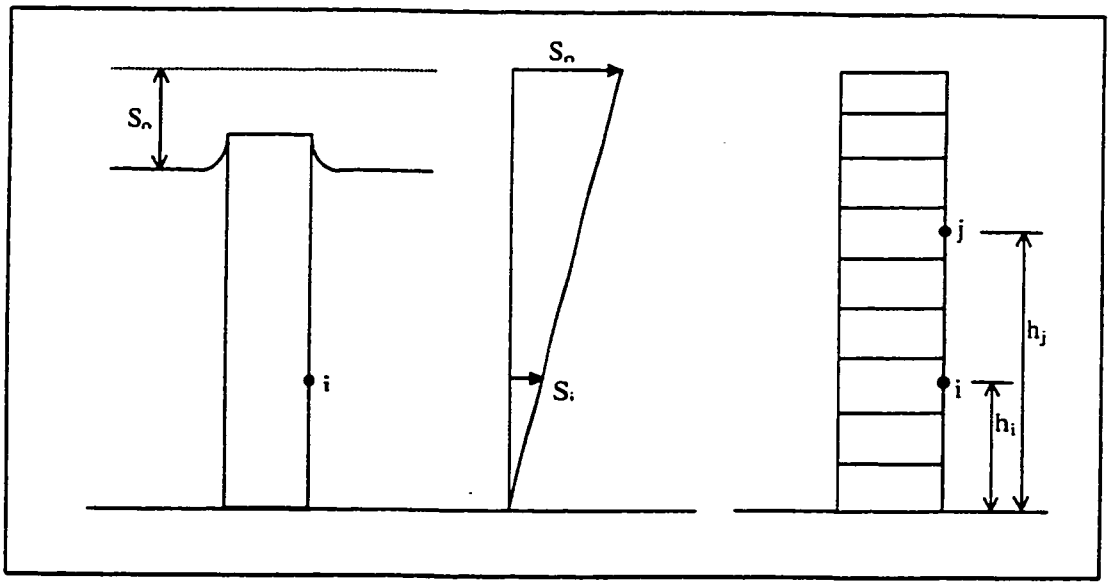

Figure (2-1) Stresses and displacements in soil-pile system, after Poulos and Mattes (1969).

It should be pointed out that this analysis is limited to end bearing piles. Furthermore, the time-dependent nature of the problem was not included in the analysis. For a more rigorous solution, a realistic profile of consolidation settlement should be adopted instead of the linear distribution of settlement assumed in the analysis.

Walker and Darvall ***(1970)*** postulated a finite element framework for determining the magnitude and distribution of negative skin friction. The pile was assumed rigid, cylindrical, and end-bearing on a rigid base surrounded by a homogenous soil. Consolidation was caused by placing surcharge at the ground surface or lowering of the ground water table. Therefore, an axisymmetrical boundary value problem was adopted for the analysis where the vertical boundary was placed at the pile tip and the horizontal boundary was placed at a remote distance from the pile surface. There was no information provided about the magnitude of this remote distance. To duplicate the field conditions, the shear stresses were considered to be zero at the remote boundary. Further, the settlement profile at the remote boundary was obtained according to the conventional consolidation theory, whereas the vertical displacement was assumed zero at the base boundary.

The surrounding soil was modeled to behave as nonlinear elastic material based on secant shear modulus (G) expressed by:

$$G(\tau) = \frac{C_2\,\tau}{\ln\left(\dfrac{C_1\,\overline{P}}{C_1\,\overline{P}-\tau}\right)} \qquad \text{and} \qquad G(\tau=0) = C_1\,C_2\,\overline{P} \qquad \ldots\ldots\ (2.5)$$

Further, the soil constitutive relationship was defined by:

$$\tau = C_1 \, \overline{P} \left(1 - e^{-C_2 \gamma}\right) \qquad \ldots\ldots \text{(2.6)}$$

where, τ = the shear stress,

$\overline{P}$ = the mean effective pressure,

γ = the shear strain,

and C_1 , C_2 = soil constants that can be determined in laboratory.

Unfortunately, there was no information provided regarding type and number of elements used in the analysis. Slippage was accounted for at the pile-soil interface when the limiting shear stress of the soil is reached. If the condition was not satisfied, the soil displacement at the interface will be set to zero. This assumption is a drawback in the analysis procedure, since the shear stresses due to elastic deformations were not included in the analysis. Therefore, a joint (slip) element should be considered to assure the continuity of the displacement along the pile-soil interface.

Bozozuk (1972) presented a semi-empirical method to determine the downdrag load for piles subjected to highway embankment surcharge. The negative skin friction was related to the horizontal effective stress acting on the pile. For such cases, the horizontal effective stress would consist of the in-situ horizontal stress, the horizontal stress due to embankment loading, the horizontal stress generated at the top of the fill by virtue of differential settlement as shown in Figure (2-2, b), and horizontal forces due to displacement of soil caused by driving closed-ended piles. The later can be neglected for non-displacement piles.

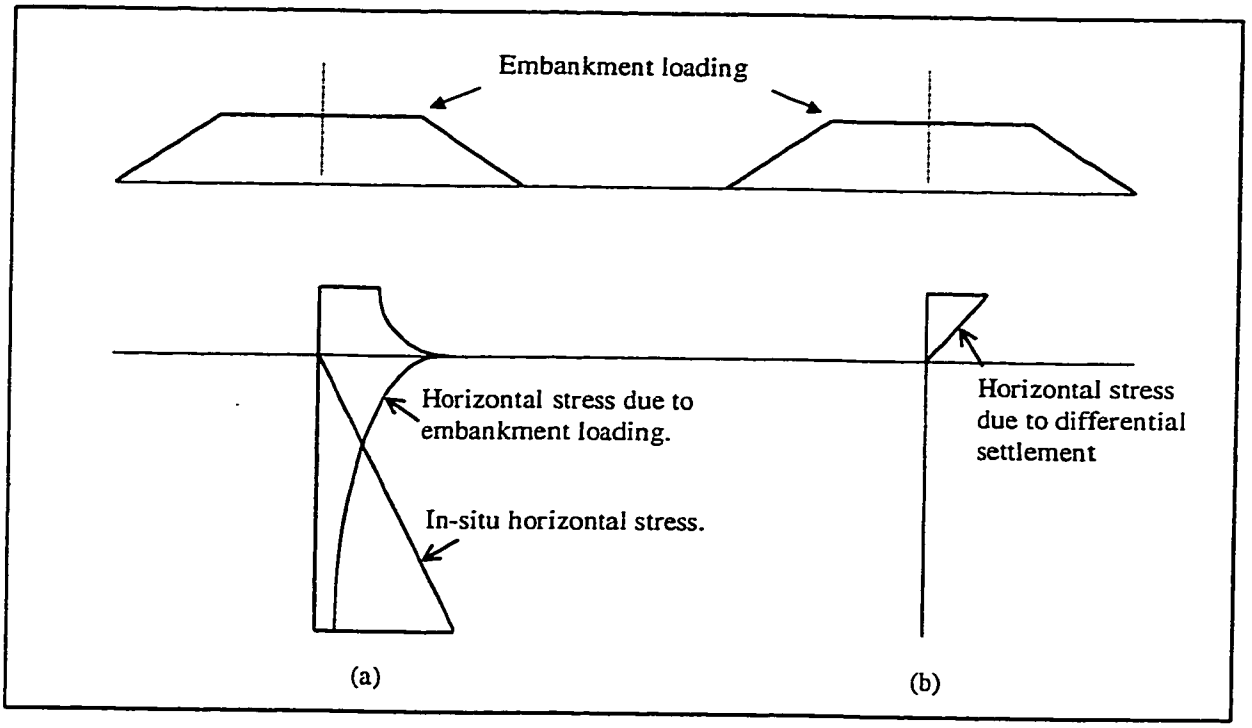

Figure (2-2) Generation of horizontal stresses under a centerline of embankment on compressible clay, after Bozozuk (1972).

To determine the downdrag load due to in-situ effective stresses, the following formula was presented

$$F_n = \int_0^{L_{NP}} MK_o(\gamma' z)\tan\phi' C\,dz \qquad \ldots\ldots (2.7)$$

where, ϕ' = the effective angle of the internal friction

γ' = submerged unit weight of the soil

K_o = coefficient of earth pressure at rest

M = friction factor for the soil acting on the pile surface, where $0 < M \leq 1$

C = circumference of the pile

L_{NP} = depth of neutral plane

The integration of equation (2.7) will yield

$$F_n = \beta_1 C \frac{L_{NP}^2}{2} \qquad \ldots\ldots (2.8)$$

where, $\beta_1 = M_{negative}\, K_o\, \gamma'\, \tan\phi'$

The negative friction load will be resisted by positive load induced in the pile from L_{NP} to the pile length, L, can be expressed as

$$Q_s = \beta_2 C \frac{\left(L^2 - L_{NP}^2\right)}{2} \qquad \ldots\ldots (2.9)$$

Neglecting the carried load by the pile tip for open-ended floating piles, then for equilibrium requirements

$$\beta_1 L_{NP}^2 = \beta_2 \left(L^2 - L_{NP}^2\right) \qquad \ldots\ldots (2.10)$$

or,

$$L_{NP} = \frac{L}{\sqrt{\eta - 1}} \qquad \ldots\ldots (2.11)$$

where, $\eta = \dfrac{\beta_1}{\beta_2}$ and $\beta_2 = M_{positive}\, K_o\, \gamma'\, \tan\phi'$

For the determination of negative friction due to horizontal stresses generated by the embankment, the same previous procedure was followed, hence

$$F_n = MC \tan\phi' \sum_{i=1}^{n_{L_{NP}}} \Delta L_i \Delta\sigma_{xi} \qquad \ldots\ldots (2.12)$$

similarly,

$$Q_s = MC \tan\phi' \sum_{i=n_{L_{NP}+1}}^{n_L} \Delta L_i \Delta\sigma_{xi} \qquad \ldots\ldots (2.13)$$

where, $\Delta\sigma x$ = average horizontal effective stress due to the embankment load acting on ΔL

The method was applied to predict the downdrag load of pipe pile floating in marine clay. A good agreement was achieved with the observed downdrag load. The distribution of the positive skin friction, however, was not in good agreement with the observed one. Bozozuk attributed this to the lack of excess pore water dissipation.

Fellenius (1972) reported that negative skin friction is a settlement problem and not a failure problem. It was further noticed that by applying temporary load to the pile head the downdrag load will reduce by a magnitude equal to the applied load. As the load became permanent, however, the negative skin friction will develop again with the continued regional settlement. It was also reported that the settlement observed to cause a full mobilization of negative skin friction was of order 2-3 mm.

Based on these observations, a general design approach was proposed to be adopted for piles subjected to downdrag loads. The approach suggests that if the transient load on the pile head is less than the downdrag load, $P_t < 2F_n$, then the permanent load on the pile will be considered, thus

$$\mathbf{P_p \leq Q_t + Q_s - F_n} \qquad \ldots\ldots \textbf{(2.14)}$$

where, P_p = the permanent load on the pile head

F_n = the downdrag load due to negative skin friction

Q_t = the ultimate tip resistance

Q_s = the ultimate positive skin resistance acting below the neutral plane

Due to the different nature of each load in the above equation, a method of partial factors of safety was adopted, hence equation (2.14) became

$$f_P P_P \leq \frac{1}{f_Q}(Q_t + Q_s) - f_n F_n \qquad \ldots\ldots \text{(2.15)}$$

where, f_p = the factor of safety on the permanent load

f_Q = the factor of safety on the ultimate bearing capacity

f_n = the factor of safety on the downdrag load

Equation (2.15) is valid if $f_P P_t < 2P_n$. It was recommended that $f_n \leq 1$ and $f_t = 2$. If the transient load was larger than twice the downdrag load, the positive skin friction will generate along the entire length of the pile. Therefore, the bearing capacity of the pile must be checked for the total load that acting on the pile, hence equation (2.15) becomes

$$f_t P_t + f_P P_P \leq \frac{1}{f_Q}(Q_t + Q_s) \qquad \ldots\ldots \text{(2.16)}$$

For end-bearing piles, either long or embedded in a settling layer thicker than 40 m., the safety factors with respect to negative skin friction should be checked by the following condition:

$$f_t P_t + f_P P_P \leq \frac{1}{f_Q'} Q_s^m \qquad \ldots\ldots \text{(2.17)}$$

where, Q_s^m = the ultimate shaft resistance acting on the full pile length

$f_Q' < f_Q$

When the downdrag load is too large to be accepted or very small pile settlement is allowed, the negative skin friction was suggested to be reduced by coating the pile with bitumen.

Poulos and Davis (1972) extended the work of Poulos and Mattes (1969) to include the effect of the rate of development of downdrag load with time in an impermeable pile. The soil was assumed to be fully saturated and to be consolidated under the action of surcharge loading. In this analysis, possibilities of local yield between pile-soil interface and limited crushing of the pile due to overloading were considered.

The problem was solved in the same manner as Poulos and Mattes (1969) except that the soil settlement considered in this analysis was due to consolidation which was obtained from a simple one-dimensional analysis. Thus, at a mid point in element i (see Fig. 2-1), the consolidation settlement was expressed as follows:

$$S_i = \Sigma\, m_v\ F_k\,(u_0 - u_t)\ L/n \qquad \ldots\ldots (2.18)$$

where m_v = coefficient of volume decrease

u_0, u_t = excess pore pressures at the point k in the soil at time of installation of the pile, and time t after installation respectively.

$F_k = 1$ for $k > i$ and 0.5 for $k = i$

The solution for the maximum downdrag load in a pile was given by:

$$F_n^m = I_N\, S\, L^2 \qquad \ldots\ldots (2.19)$$

where I_N = the influence factor

S = the surcharge pressure

L = the pile length

To obtain the final downdrag force, the maximum downdrag load (F_n^m) must be corrected by multiplying it by number of factors, namely: correction factor for cases in which full slip does not occur, for effects of delayed installation after consolidation has been permitted, and for soil Poisson's ratio greater than zero.

Although the solution provided by the authors was limited to end-bearing piles, the analysis could be extended to allow for finite base compressibility, and for the case of consolidation under own weight, provided that large strains do not occur.

Feda (1976) advocated the use of the initial undrained shear strength to evaluate skin friction for single piles embedded in both clays and sands. The method is also applicable for piles subjected to residual stress due to either loading history and/or method of installation. The fundamental assumption of the method was that the soil around the middle part of the pile shaft will experience no volume change during loading. This is analogous to the undrained condition in a sense that both possess no volume change. Thus the pile-soil interaction was modeled by a direct shear test where the volume of the sample was kept constant. It was illustrated by the results of the constant volume shear test that the shear resistance under confined conditions is independent of the initial normal stress and depends only on the initial porosity.

Negative skin friction was introduced as a cause of residual stresses. It was shown that the skin friction is negative at the upper part and positive at the lower part of the pile, as illustrated in Figure (2-3). The relative displacement between the pile and the ambient soil was attributed to two components. The first is due to the elastic rebound of the soil at the pile base displacing the pile upward. The second component is the elastic elongation of the pile itself which attains its maximum near the pile head and decreases downwards. Expressions to determine the neutral depth, the average negative skin friction, and the average positive skin friction were presented as follows:

$$L_{NP} = \frac{L\tau_{pr} + \frac{\zeta P_m}{\pi D}}{\tau_{nr} + \tau_{pr}} \qquad \ldots\ldots \text{(2.20)}$$

and in case of isotropic skin friction (i.e. $\tau_{nr} = \tau_{pr}$)

$$L_{NP} = \frac{L}{2} + \frac{\zeta P_m}{2\pi D\,\tau_{pr}} \qquad \ldots\ldots \text{(2.21)}$$

where, L_{NP} = depth of neutral point

L = length of the pile

D = diameter of the pile

τ_{pr} = positive residual skin friction

τ_{nr} = negative residual skin friction

P_m = maximum load previously applied on the pile head

$\zeta = \frac{P_r}{P_m}$; where P_r = residual load at the pile tip

for average negative skin friction:

$$\bar{\tau}_n = \tau_n^m - \frac{\zeta P_m}{\pi DL} \qquad \ldots\ldots \text{(2.22)}$$

and for the average positive skin friction:

$$\bar{\tau}_p = \tau_p^m + \frac{\zeta P_m}{\pi DL} \qquad \ldots\ldots \text{(2.23)}$$

where, τ_n^m and τ_p^m = the maximum negative and positive skin friction respectively.

An important conclusion can be drawn from the above skin friction relationships is that for an: (i) isotropic skin friction ($\tau_n^m = \tau_p^m$), $\bar{\tau}_n \cong \bar{\tau}_p$ in case of bored piles ($\zeta \cong 0$), and $\bar{\tau}_n << \bar{\tau}_p$ in case of driven or jacked piles ($\zeta > 0$). (ii) anisotropic skin friction by

virtue of deformation anisotropy caused by the method of installation of piles ($\tau_n^m > \tau_p^m$) , $\bar{\tau}_n > \bar{\tau}_p$ in case of bored piles with driven casing ($\zeta \equiv 0$), and in case of driven or jacked piles ($\zeta > 0$) $\bar{\tau}_n \equiv \bar{\tau}_p$.

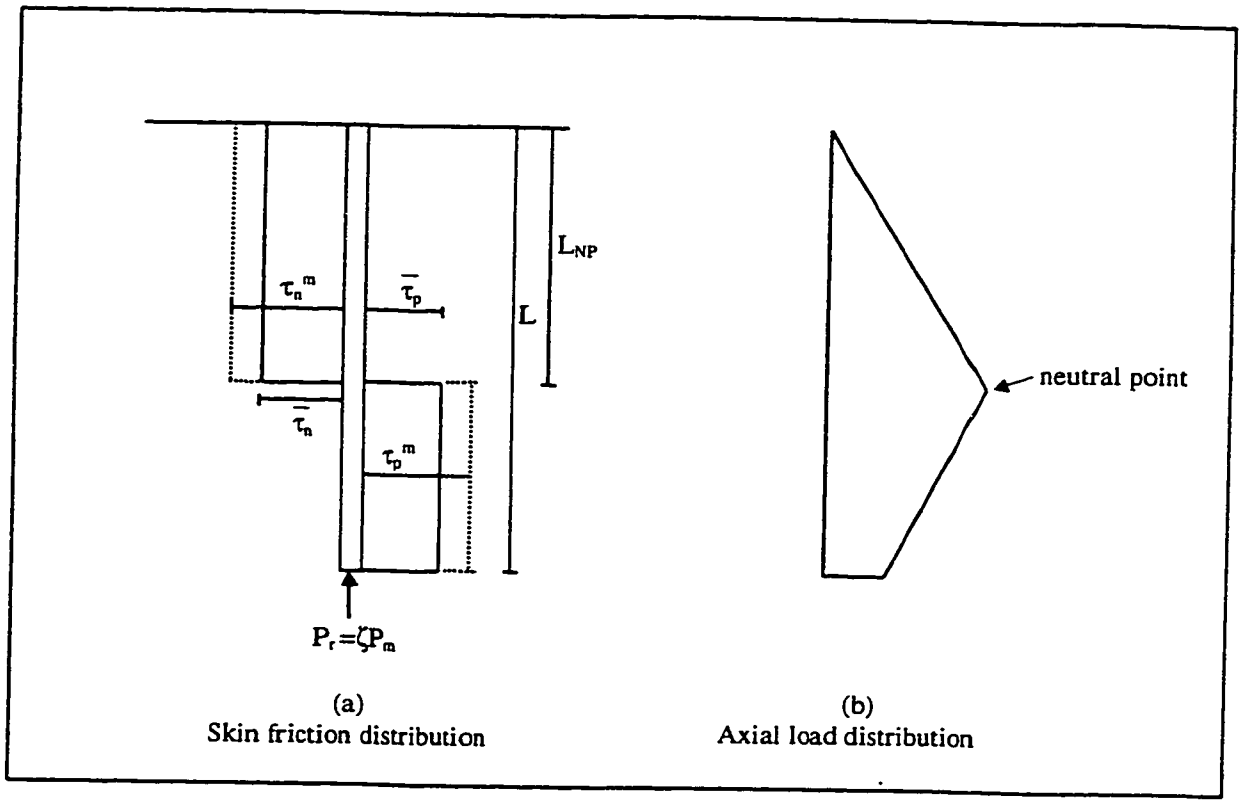

Figure (2-3) A schematic diagram of the residual skin friction and tip load of a pile, after Feda (1976).

Janbu (1976) presented a theoretical method for determining the bearing capacity of friction piles. For piles subjected to pull out or embedded in settling soil to rock, the negative skin friction can be estimated by

$$\tau_n = S_n (P_z + a) \qquad \ldots\ldots \text{(2.24)}$$

where, S_n = negative skin friction number

P_z = effective stress at depth z

$a = c \cot\phi$ (soil attraction)

c = cohesion

ϕ = angle of shearing resistance

An expression for the negative skin friction number was developed which can be written as:

$$S_n = |r_n| \mu K_s \quad \ldots\ldots \text{(2.25)}$$

where, r_n = the roughness number

$\mu = f \tan\phi$, mobilized skin friction, where f is the degree of mobilization

K_s = the earth pressure coefficient

The only available solution provided for K_s was limited to plane strain condition, which reads:

$$K_s = \left(\sqrt{1+\mu} + \mu\sqrt{1+r_n}\right)^{-2} \quad \ldots\ldots \text{(2.26)}$$

The roughness number was considered as a product of two factors: (a) the mechanical roughness of the pile surface and (b) the relative movement between the pile and the adjacent soil. Thus for very long piles, the roughness number will decrease dramatically with pile's depth as can be seen from Table (2.1).

Table (2.1) presents the recommended values for (r_n) with corresponding depth.

z (m)	0	5	10	20	50	100
r_n	1.0	0.9	0.8	0.7	0.6	0.5

Fleming et. al. (1985) extended the work of Randolph and Wroth (1978) to include the determination of the distribution of negative skin friction on the pile's shaft. The method is basically a load transfer approach which involves the hypothesis of considering the pile to be surrounded by concentric soil cylinders having shear stresses induced on each with magnitudes decreasing inversely with surface area of the cylinders. Thus the shear stress at distance (r) from the pile center can be expressed by the following:

$$\tau_r = \frac{\tau_o r_o}{r} \qquad \ldots\ldots (2.27)$$

where, τ_r = the shear stress at radius r

τ_o = the shear stress on the pile shaft

r_o = the radius of the pile.

Since the main deformation in the soil will be vertical, the shear strain may be written, in polar cylindrical coordinates, approximately as:

$$\gamma \cong \frac{dw_s}{dr}$$, where w_s = the vertical soil displacement

then, by introducing the shear strain, equation (2.27) can be written as:

$$w_p = \int_{r_o}^{r_m} \frac{\tau_o r_o}{G r} dr = \frac{\tau_o r_o}{G} \zeta \qquad \ldots\ldots (2.28)$$

where, w_p = the deflection of the pile

r_m = the maximum radius at which the deformation can be ignored

G = the shear modulus of soil

ζ = $\ln(r_m/r_o)$, varies between 3 to 5 with an average value of 4.

Having introduced the foregoing, and knowing that negative skin friction is generated by the relative displacement between the pile and the surrounding soil, the local shear stress on the pile shaft for small relative movements can be written as follows:

$$\tau_o = \frac{G}{\zeta r_o}(w_o - w_s) \qquad \ldots\ldots \text{(2.29)}$$

where, w_s = the settlement of the surrounding soil

w_o = the local settlement of the pile

the pile settlement was given by:

$$w_o = w_b + \int_0^L \frac{P}{(AE)_p} dz \qquad \ldots\ldots \text{(2.30)}$$

where, w_b = the settlement of the pile tip

L = the pile length

A = the cross-sectional area of the pile

E = the pile modulus of elasticity

P = the axial load transferred to the pile, which can be estimated from:

$$P = P_h - \int_0^L 2\pi r_o \tau_o \, dz \qquad \ldots\ldots \text{(2.31)}$$

where, P_h = the applied load on the pile head.

Considering the pile base as a rigid punch acting on a surface of soil medium, the base settlement can be obtained from

$$w_b = \frac{P_b(1-\nu)}{4 r_o G_b} \qquad \ldots\ldots \text{(2.32)}$$

where, P_b = the load carried by the pile tip

ν_s = Poisson's ratio of the soil

For the relative movements equal to or greater than the one that is necessary to cause slip, the fully mobilized shear stress may be estimated by:

$$\tau_s = K_o \sigma'_v \tan\phi' \qquad \ldots\ldots (2.33)$$

where, K_o = coefficient of earth pressure at rest, which may be taken as $(1 - \sin\phi')$

σ'_v = the vertical effective stress

ϕ' = the effective angle of the internal friction

thus if $| w_o - w_s | \geq w_{slip}$ then (τ_o) in equation (2.29) will be equal to (τ_s), where

$$w_{slip} = \frac{\tau_s r_o}{G} \zeta \qquad \ldots\ldots (2.34)$$

It is obvious that the method requires some iteration in order to assess the distribution of the negative skin friction. It further requires information on the soil settlement profile due to consolidation.

Van Der Veen (1986) Cited the importance of considering the pile settlement as a relevant design aspect for piles subjected to negative skin friction. The effect of the allowable settlement on the allowable bearing capacity was demonstrated by discussing three cases of piles driven into a clay layer, (a) end-bearing piles, (b) floating piles, and piles resting on a less compressible layer (such as a loose sand layer). The first two cases were considered as extreme cases as compared to the third one to which most of the discussion was devoted.

A general design formula was proposed to determine the allowable bearing capacity in which the settlement effect was accounted for. This formula reads as follows,

$$P_a = \frac{Q_t}{f_s} - \lambda F_n^m \qquad \ldots\ldots \text{(2.35)}$$

where, P_a = the allowable bearing capacity

Q_t = the ultimate bearing capacity of the pile tip including the positive skin friction generated in the less compressible layer in which the pile tip is resting

f_s = the factor of safety related to the allowable settlement

F_n^m = the maximum negative friction load in case of end-bearing piles assuming that the negative skin friction is fully mobilized along the pile shaft

λ = negative skin friction coefficient

The negative skin friction coefficient, λ, is a multiplication component of two factors, the reduction number,η, and the condition number, ζ. The reduction number, η, varies between 0.7 and 0.9. It reflects the effect of the reduction of the effective overburden pressure in the vicinity of the pile shaft, which was expressed by

$$\eta = \frac{1}{1 + K_o \tan\phi'} \qquad \ldots\ldots \text{(2.36)}$$

where, K_o = the coefficient of earth pressure at rest, and can be taken as $(1-\sin\phi')$

ϕ' = the effective angle of shearing resistance.

On the other hand, the condition number, ζ, depends on the pile settlement relative to the compressible soil. For piles extended through compressible layers into moderate to very firm sand, ζ varies between 0.5 and 1.0.

The allowable bearing capacity computed from equation (2.35) should be compared with the one determined from the following expression

$$P_a = \frac{Q_t + Q_s^m}{FS} \qquad \ldots\ldots (2.37)$$

where, Q_s^m = the ultimate shaft resistance acting along the full pile length

FS = the factor of safety in terms of the ultimate bearing capacity

The lower of the two values, obtained from equations (2.35) and (2.37), is finally the allowable bearing capacity of the pile.

Fellenius (1989) pointed out that not only those embedded in compressible soils, but all piles experience negative skin friction. This conclusion was based on the fact that a movement of as small as 1-2 mm. is sufficiently enough for full mobilization of skin friction, bearing in mind the considerable deference in rigidity between a pile and soil in which such a small relative movement may occur.

A unified design approach was therefore proposed in which bearing capacity, pile's structural capacity, and pile settlement were all taken in consideration. The neutral point must first be located. Then the structural capacity of the pile is checked. The settlement is next determined by applying the concept of an equivalent footing placed at the neutral plane. Finally the bearing capacity is verified.

Each design step has a combination of loads that should be used in its computation. The pile structural capacity at the pile cap level is checked by a combination of dead and live loads, whereas at the neutral point level dead and downdrag loads are

considered, but the live load is excluded. For bearing capacity computation, dead and live loads are considered, but the downdrag load is omitted. Neither live nor downdrag loads, only dead load should be considered in settlement calculation.

The neutral plane was suggested to be determined by constructing two load distribution curves. The first, combining both the dead and downdrag loads, is drawn starting from the pile head and being considered as acting along the entire length of the pile. Then starting from the pile tip, the second curve is drawn with the values of the tip resistance and the positive skin friction. Thus the neutral point is located at the intersection of the two curves.

Lim et al (1993) described a simple discrete element approach utilizing the subgrade reaction method to analyze negative skin friction on single piles. The pile was assumed to be embedded in a two-layer soil where the upper soil layer undergoes consolidation while the lower layer performs as a stiff bearing stratum. The analysis takes into account the effect of socketed piles in the bearing layer. Galerkin method was applied to transform the following governing equation into discrete element formulation

$$-E_p A \frac{\partial^2 w}{\partial z^2} + k(w - w_s) = 0 \qquad \ldots\ldots \text{(2.38)}$$

where, E_p = the elastic modulus of the pile material

A = the cross-sectional area of the pile

w_p = the axial deformation of the pile

w_s = the soil consolidation settlement of soil

k = the soil stiffness per unit pile length

The soil stiffness, k, was determined based on the assumption that the deformation modes of the soil along the pile shaft and at the pile tip are uncoupled. The deformation modes were estimated according to the solution provided by Randolph and Wroth (1978), see equations (2.28) and (2.32). Thus, the expression adopted for the soil stiffness at the pile shaft, k, and at the pile tip, k_{base}, were as follows

$$k = 2\pi \frac{G}{\ln\left(r_m / r_o\right)} \qquad \ldots\ldots \text{(2.39)}$$

and

$$k_{base} = \frac{4 G_b r_0}{(1-\nu_b)} \qquad \ldots\ldots \text{(2.40)}$$

where, G, G_b = the shear modulus of the compressible layer and the bearing layer respectively

ν_b = Poisson's ratio of the soil at the base

r_o = the pile radius

r_m = the maximum radius of influence at which shear stresses become negligible.

The influence radius, r_m, was considered to vary linearly with depth as shown in Figure (2-4). Based on a comparison study with other rigorous methods, empirical solutions were developed for r_m, in which socketed piles were taken into account, to be adopted in the analysis. For practical purposes, r_m was recommended to be taken as a stepwise constant. It should be pointed out that the analysis described here provides basically an elastic solution; therefore, this method should be used with caution when excessive consolidation settlement is expected.

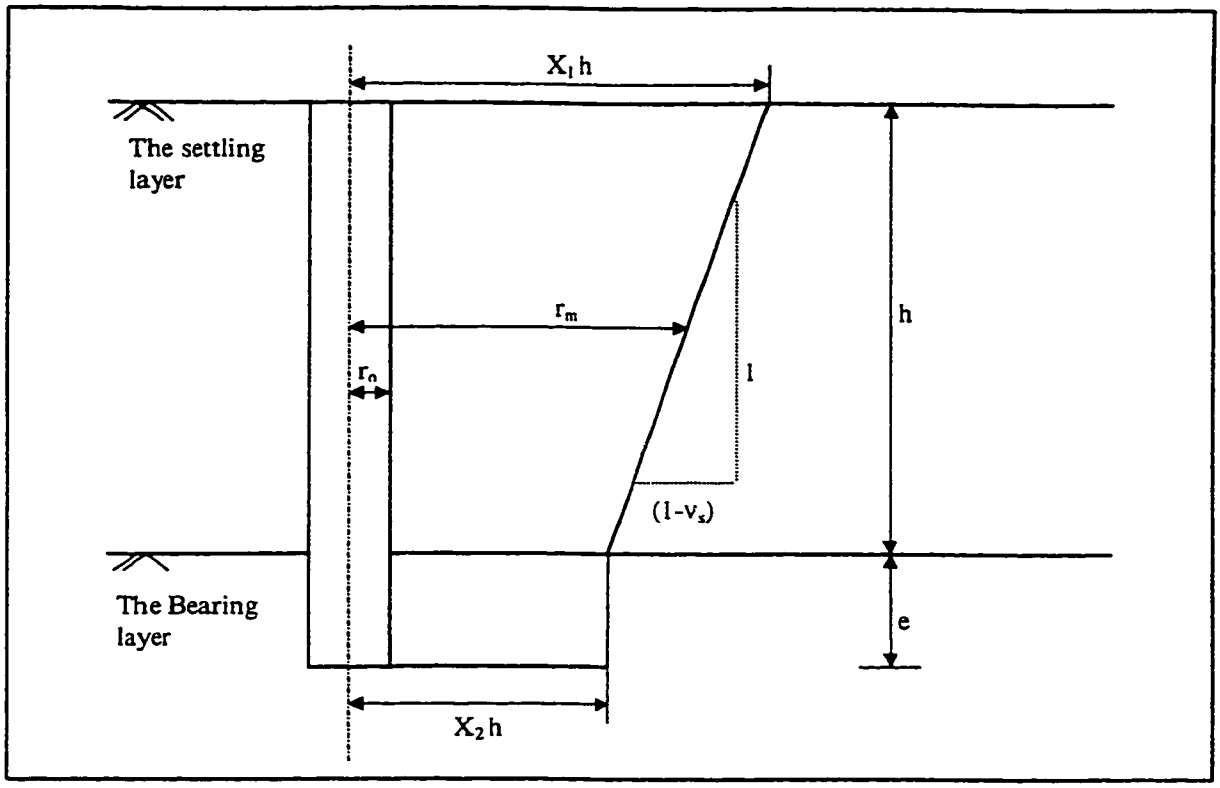

Figure (2-4) The variation of r_m with depth for a pile embedded in a two-layer soil, after Lim et al (1993).

Matyas and Santamarina (1994) developed two closed-form solutions for determining the downdrag load and the neutral point location. The first solution was based on modeling the soil-pile interface as a simple rigid-plastic material, whereas in the second solution the interface was modeled as elastic-plastic material. The pile was assumed to be rigid and embedded in a medium with linearly increasing shaft resistance. By comparing the two solutions, it was found that the rigid-plastic solution may overestimates the downdrag load by as much as 50% or more, and overpredicts the location of neutral depth by about 30%.

In the rigid-plastic model, the negative skin friction, the positive shaft resistance, and the tip resistance were assumed fully mobilized. It was further assumed that the unit negative skin friction, q_n, is equal to the unit positive skin friction, r_s. To preserve generality, two dimensionless ratios were introduced: $\alpha = \frac{Q_u}{Q_s}$ and $FS = \frac{Q_u}{Q_d}$, where Q_u is the ultimate bearing capacity, Q_s is the ultimate shaft resistance, and Q_d is the allowable (dead) load. Thus for equilibrium requirements:

$$Q_d + \int_0^{L_{NP}} A_s q_n \, dz = \int_{L_{NP}}^{L} A_s r_s \, dz + Q_t \qquad \ldots\ldots \text{(2.41)}$$

where, A_s = the area of the shaft surface

L = the length of pile

L_{NP} = the depth of neutral plane

Q_t = the ultimate resistance of the pile tip

By integrating and rearranging equation (2.41), the following expressions can be reached:

$$\frac{L_{NP}}{L} = \sqrt{\frac{\alpha}{2}\left(\frac{FS-1}{FS}\right)} \qquad \ldots\ldots \text{(2.42)}$$

$$\frac{Q_{NP}}{Q_u} = \frac{(1+FS)}{2FS} \qquad \ldots\ldots \text{(2.43)}$$

where, Q_{NP} = the total load at the neutral plane depth

For elastic-plastic method, the relative displacement profile was assumed linear, with maximum value at the ground surface and decreasing with depth, as shown in Figure(2-5). Three additional dimensionless ratios were introduced: $\Psi = \frac{\delta_{ty}}{S_t}$, $\omega = \frac{\delta_{sy}}{S_t}$,

and $\lambda = \frac{\delta_h}{S_t}$, where δ_{sy} is the relative displacement between the pile and the soil required for yielding the shaft resistance, δ_{ty} is the relative displacement that yields the tip resistance, δ_h is the settlement of the pile head, and S_t is the total relative settlement.

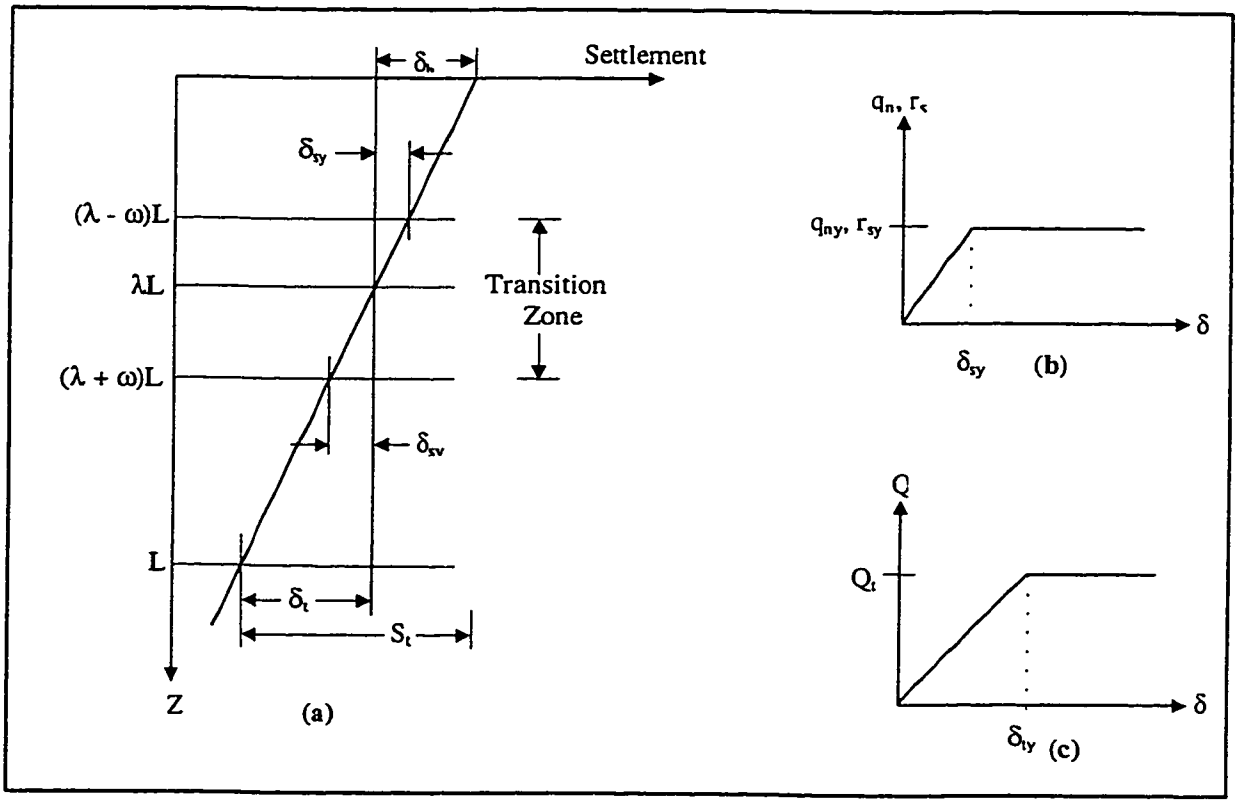

Figure (2-5) Elastic-plastic model. (a) The relative displacements. (b) Mobilization of shaft resistance. (c) Mobilization of tip resistance. After Matyas and Santamarina (1994)

Similarly, by equating the forces above the neutral point with those which are below, the following expressions were reached:

$$\frac{L_{NP}}{L} = \frac{\sqrt{(\alpha-1)^2+8\psi(\alpha-1)+8\psi^2\left(1-\frac{\alpha}{FS}-\frac{2\omega^2}{3}\right)}-(\alpha-1)}{4\psi} \quad \ldots\ldots (2.44)$$

$$\frac{Q_{NP}}{Q_u} = \frac{1}{\alpha}\left(\lambda^2-\lambda\omega+\frac{1}{3}\omega\right)+\frac{1}{FS} \quad \ldots\ldots (2.45)$$

During the comparison of the two solutions, the elastic-plastic method estimated neutral depth values for rigid and deformable end-bearing layers that contradict with the physical evidence. It gave identical values of neutral plane depths for the two cases. These equations, therefore, are not recommended to be used for practical purposes.

Wong and Teh (1995) proposed a numerical procedure for the analysis of the negative skin friction on piles in layered soil deposit. The pile-soil interface was modeled by a series of nonlinear soil springs. The soil spring was governed by the following hyperbolic equation

$$P_i = \frac{w_i}{\left(\frac{1}{k_{si}}+\frac{w_i}{P_{ui}}\right)} \quad \ldots\ldots (2.46)$$

where, P_i = the nodal force

k_{si} = the initial tangent of the hyperbolic curve

w_i = the relative pile-soil settlement

P_{ui} = the maximum nodal load given by, $P_{ui} = f_{si} \cdot A_{si}$

where, f_{si} is the limiting unit shaft friction and A_{si} is the shaft area associated with the node i

For the pile shaft, the initial spring stiffness, k_{si}, adopted was based on the relationship derived by Randolph and Wroth (1978) given by

$$k_{si} = \frac{2\pi G_i l_i}{\ln\left(\frac{r_m}{r_o}\right)} \qquad \ldots\ldots (2.47)$$

where, G_i = the soil shear modulus

l_i = the pile segment length

r_m = the radius of the influence zone

r_o = the pile radius

For Gibson's soil in which the stiffness increases with depth, the expression for r_m proposed by Lee (1993) was adopted

$$r_m = 2(1-\nu_s)L \int \frac{G_{iz}}{G_b L} dz \qquad \ldots\ldots (2.48)$$

where, ν'_s = the soil Poisson's ratio

L = the pile length

G_{iz} = the soil shear modulus at depth z

G_b = the soil shear modulus at the pile tip

The initial tangent for the spring at the pile tip, k_{ti}, was based on the solution of a rigid punch on a semi-infinite elastic half-space, given by

$$k_{ti} = \frac{4 G_b r_o}{(1-\nu_s)} \qquad \ldots\ldots (2.49)$$

A hybrid incremental-iterative procedure was employed to allow for large incremental steps without compromising on the accuracy of the solution. A consistent procedure was established to estimate the input parameters from conventional soil test data.

This procedure was used in back-analysis of seven well-documented test piles in different soil deposits. The results of the analysis showed that the numerical approach is capable of predicting the downdrag loads with reasonable accuracy.

Esmail (1996) conducted a parametric study on single piles subjected to negative skin friction due to surcharge loading. The numerical modeling was based on finite element technique utilizing two soil constitutive models, Modified Cam-Clay model and elastic-plastic model with Mohr-Coulomb yielding criterion. The soil was allowed to consolidate under the effect of surcharge loading. In the Mohr-Coulomb model, the strength parameter was introduced in terms of the undrained condition. Based on the parametric study, design charts for the Modified Cam-Clay and Mohr-Coulomb models were developed to determine the neutral depth.

Poorooshasb et al (1996) presented a numerical scheme that can be used to evaluate the magnitude and distribution of the negative skin friction. It also can handle material non-linearity, time dependency, and both end-bearing and floating piles. The numerical analysis starts with developing an integro-differential equation which can be solved numerically by introducing it in a finite difference form suitable for computer coding. The integro-differential equation (2.50) was constructed by substituting the stress components in the incremental equilibrium equation in terms of the vertical displacement (w).

$$\frac{\partial w}{\partial z}+f(z)\int_0^z\left[g(\xi)\frac{\partial^2 w(r,\xi)}{\partial r^2}+\frac{1}{r}\frac{\partial w(r,\xi)}{\partial r}\right]d\xi - f(z)P_o = 0 \qquad \ldots . (2.50)$$

where f (z) = a soil parameter similar to the inverse of modulus of elasticity

g (z) = a soil parameter similar to the shear modulus.

It should be noted that the equilibrium is satisfied only globally, and hence the analysis yields an upper bound solution.

As a demonstration to the capability of the numerical procedure, a study on the behavior of the negative skin friction for both floating and end bearing piles was conducted. The study showed that the neutral depth was not prominently influenced by the height of the fill as suggested by the equation proposed by Bowles (1982) to determine the neutral depth, but the presence of a strong layer at the pile tip would have the major effect.

2.3 DISCUSSION

The above work can be categorized into three broad categories, namely, semi-empirical and closed form solutions, general design formulae and procedures, and numerical methods.

In the first category, the semi-empirical solutions determine the downdrag load by integrating the negative skin friction above an assumed neutral plane depth or above a rigid bearing stratum. The negative skin friction is calculated based on empirical factors that relates the unit negative skin friction to either the initial effective overburden pressure or to the initial undrained strength. The neutral plane depth is located according to

practical judgment or from an equation which is based on equilibrium that excludes the settlement effect. Most of the closed form solutions are limited to end bearing piles. The rest were developed to be used as a mean of a comparison study to emphasize the importance of an assumption over another without being verified with field data or further investigation.

The general design approaches involve a lot of debatable opinions in particular those related to the estimation of bearing capacity. Some suggests that the downdrag load should not be included in the determination of bearing capacity. The others include the downdrag load in the bearing capacity computation, but the downdrag load used is reduced either by a factor of safety or by a friction number. They all agree, however, on the involvement of settlement as a relevant design aspect.

The numerical methods were developed essentially for the need to overcome the limitations involved in the empirical methods, such as the inability in estimating the exact location of neutral point, the pile settlement, and the rate of downdrag development during consolidation. The design charts and equations produced by some of the analytical methods are limited to end-bearing piles. Most of the analytical methods require further study and refinement especially toward the input parameters.

It is obvious from the above that further research is required on this subject. Furthermore, the solution desired for practical purposes should preserve simplicity, but compromises with realistic assumptions. This can be achieved by developing design charts easy to use, and requires less number of input parameters that can be determined from conventional soil testing. It further can be inferred from the above that the determination of neutral depth is very important for computing bearing capacity and settlement of piles.

CHAPTER 3
NUMERICAL MODELING

3.1 GENERAL

The finite element method is the most popular method in engineering science. It has been successfully applied to a large number of problems in widely different fields. It started with structural applications where the applied loads were related to the displacements, through which the physical meaning of the method steps were presented to solve classical load-deformation problems.

The basis of the method involves representation of a continuum by an assemblage of subdivisions of arbitrary shapes called finite elements. These elements are held together by joints known as nodes. The displacements within each element can be calculated by introducing a set of functions called shape functions or interpolation function provided that the nodal displacements are known.

The principle of virtual work is usually used to derive the element stiffness matrix and the element nodal forces vector. Taking into account the overall equilibrium of the internal and external work done, a finite element equation of the assemblage is formulated to be solved for displacements at every element nodes in the continuum. Then, by introducing a suitable constitutive law, the stress and strain components can be computed at any location within an element by using the solved nodal displacements.

3.2 THE NUMERICAL MODEL

3.2.1 Type and Size of the Finite Element Mesh

Since both geometry and loading is symmetrical about the pile's vertical axis, the problem is reduced to a two dimensional one. Therefore, an axisymmetrical analysis was adopted throughout this investigation.

The mesh size is usually determined by the pile size and the amount of deformation expected during the analysis. For a mesh to be of sufficient accuracy, Trochanis et al. (1988) suggested that the mesh bottom should be placed at a distance of 0.6 to 0.7 times the pile length (L) from the pile tip, and placing the lateral boundary at a distance of 0.6L from the pile's center axis. Whereas, Randolph (1975), based on a comparison with boundary element method, proposed that the lateral boundary should be placed at a distance of 25 times the pile diameter (D) from the pile's center axis, and placing the mesh bottom at a distance of 1.5L from the pile's tip.

Making use of the foregoing two suggestions, the mesh size adopted herein is as shown in Figure (3-1). The lateral boarder is placed at a distance of either 0.6L or 25D, what ever is farther, from the pile shaft. The mesh bottom is placed at a distance of 0.7L. The mesh is designed to be denser in the vicinity of the pile, where the deformations and the stresses expected to vary very quickly. This zone is subdivided in a way that degree of accuracy is compromised with computational cost. Hence, its boundary starts from the pile shaft to the higher of either 0.24L or 10D horizontally, and 0.2L from the pile tip vertically.

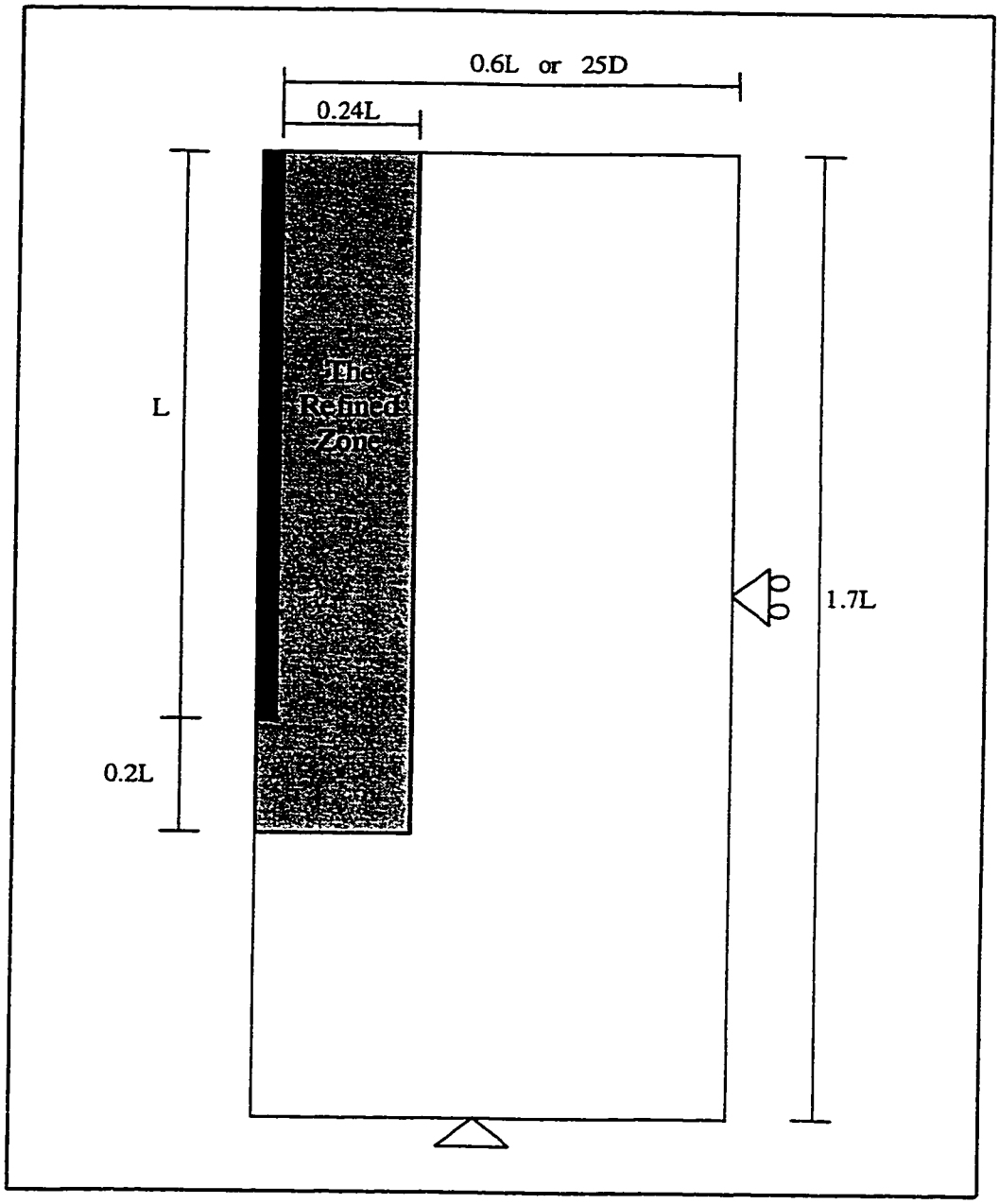

Figure (3-1) Size and boundary conditions of the finite element mesh

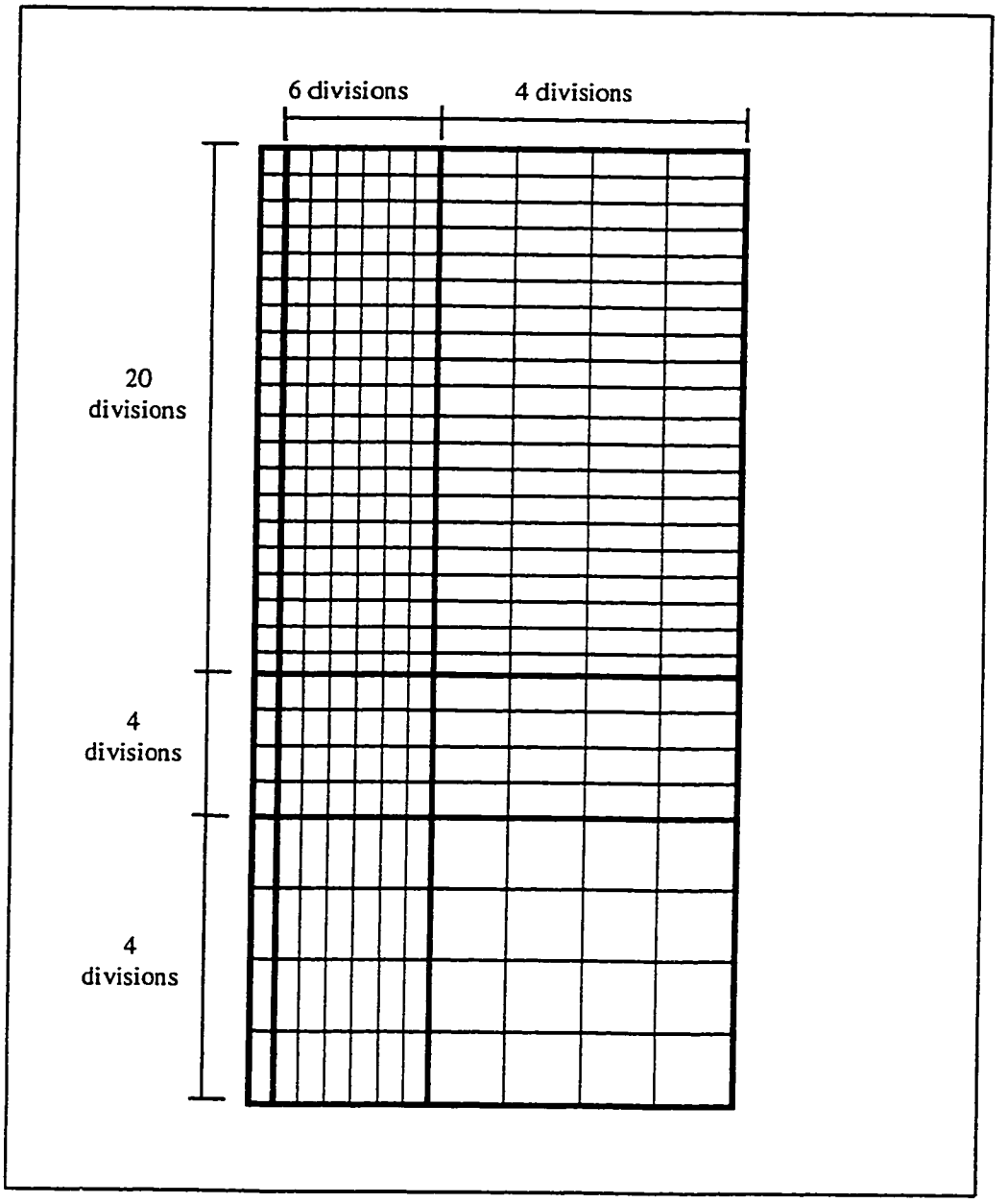

Figure (3-2) The elements' distribution in the finite element mesh

It should be noted that accuracy can be obtained with coarser meshes when the tip load is not expected to be a controlling factor in the analysis (Trochanis et al., 1988). Thus, a mesh division of 329 elements and 370 nodes was found sufficiently enough for the current analysis as shown in Figure (3-2).

3.2.2 Type of Elements

The pile is modeled by an eight nodded linear strain quadrilateral element, whereas the soil is modeled by the previous element but with linearly varying excess pore pressure. A thin layer element (slip element) is also used to model the soil - pile interface; a further discussion on this element will take place later herein. Figure (3-3) shows a schematic diagram of the used elements.

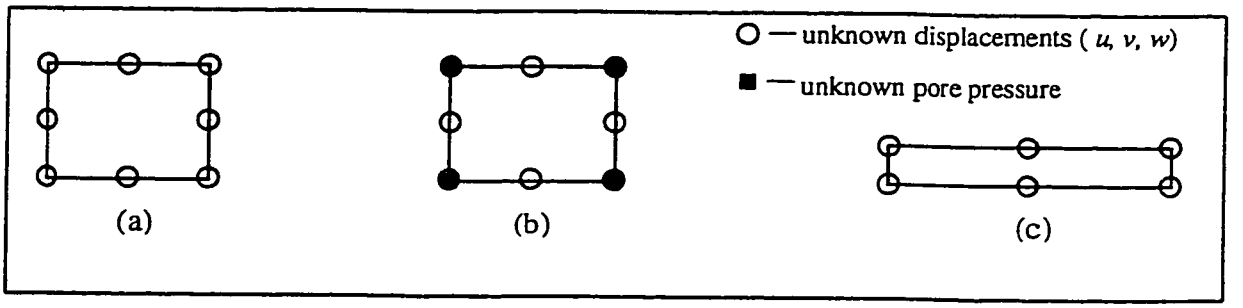

Figure (3-3) Types of elements used in the analysis. (a) Element type used for pile. (b) Element type used for soil. (c) The slip element.

3.2.3 Boundary Conditions

It is well known that one of the major drawbacks of finite element modeling is when it deals with infinite domain problems. Thus in such cases, boundary conditions

should be chosen and placed carefully to represent the entire domain in terms of in-situ stresses and displacements.

The boundaries, therefore, are placed as far as possible, as specified in section 3.2.1, at which stresses and strains have no effects in the restrained directions. Moreover, the lateral boundaries were restrained only in the (x) direction so consolidation can be permitted to take place. The bottom of the mesh, where no major displacements expected to take place, was restrained in both (x) and (y) directions, as shown in Figure (3-1).

3.2.4 The Pile Model

The pile elements were considered to behave as linearly elastic material throughout the analysis. The pile properties and their values that were used in the current study are as follows:

$E_P = 20{,}000{,}000$ kPa.

$\nu_p = 0.33$

$\gamma_p = 24$ kN/m^3

Four different pile lengths were considered in the analysis; namely, 15, 30, 45, and 60 m, and four slenderness ratios (L/D) were also used, which are: 25, 50, 75, 100.

3.2.5 The Soil Model

The soil was modeled to behave as a linear elastic-perfect plastic material, and its yield function is defined by Mohr-Coulomb criterion.

This model was selected because of its reasonable accuracy, simplicity, and widely used in practice. The criterion of Mohr is defined by the following relationship:

$$\tau = f(\sigma) \qquad \ldots\ldots\ldots (3.1)$$

where the limiting shear stress, τ, in a plane depends only on the normal stress, σ, acting in the same plane. Furthermore, the normal stress function, $f(\sigma)$, represents the failure envelope for the corresponding Mohr's circles, as shown in Figure (3-4).

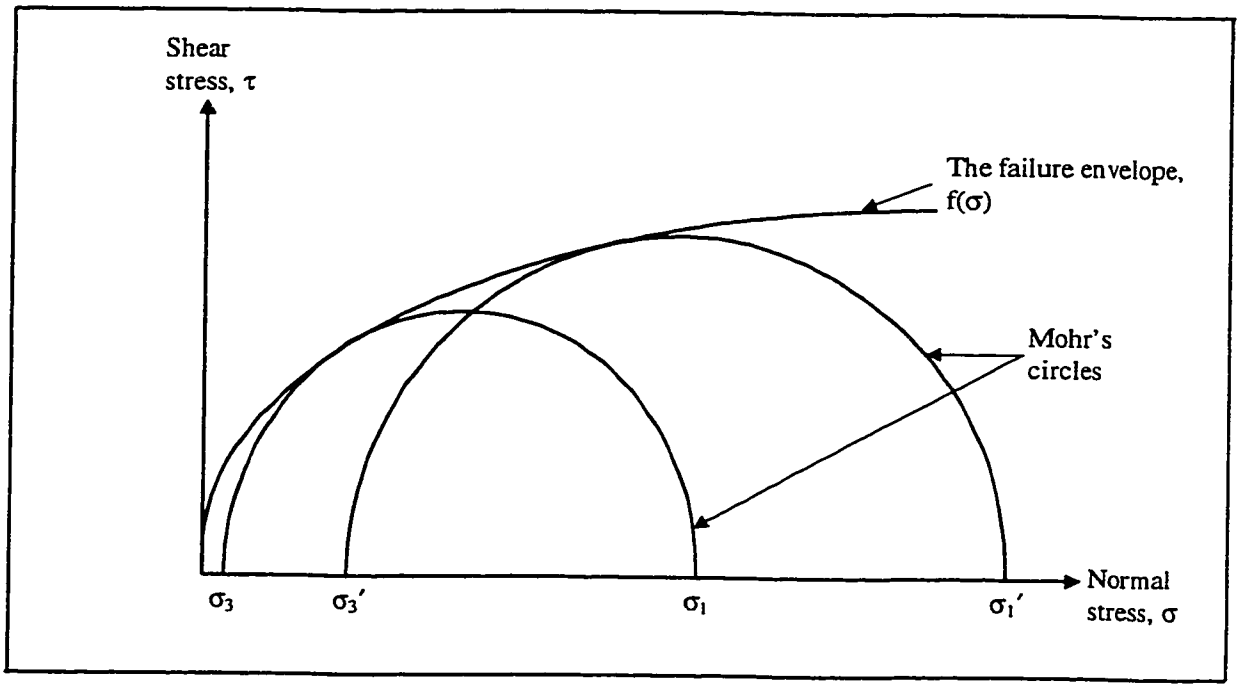

Figure (3-4) Mohr-Coulomb failure envelope

Coulomb, much earlier, introduced his well known equation,

$$\tau = c + \sigma \tan(\phi) \qquad \ldots\ldots\ldots (3.2)$$

which is considered to be the simplest form of Mohr Failure envelope, where (c) and (ϕ) are the strength parameters of the material; (c) represents the soil cohesion and (ϕ) represents the angle of soil shearing resistance. The Mohr Failure criterion associated with Coulomb equation is referred to as the Mohr - Coulomb criterion. Figure (3-5)

shows the Mohr - Coulomb failure trace in a deviatoric plane. The failure surface can be expressed in terms of principle stresses as follows:

$$\sigma_1 \frac{(1-\sin\phi)}{2c\cos\phi} - \sigma_3 \frac{(1+\sin\phi)}{2c\cos\phi} = 1 \qquad \ldots\ldots \text{(3.3)}$$

where σ_1 and σ_3 are the major and minor principal stresses respectively.

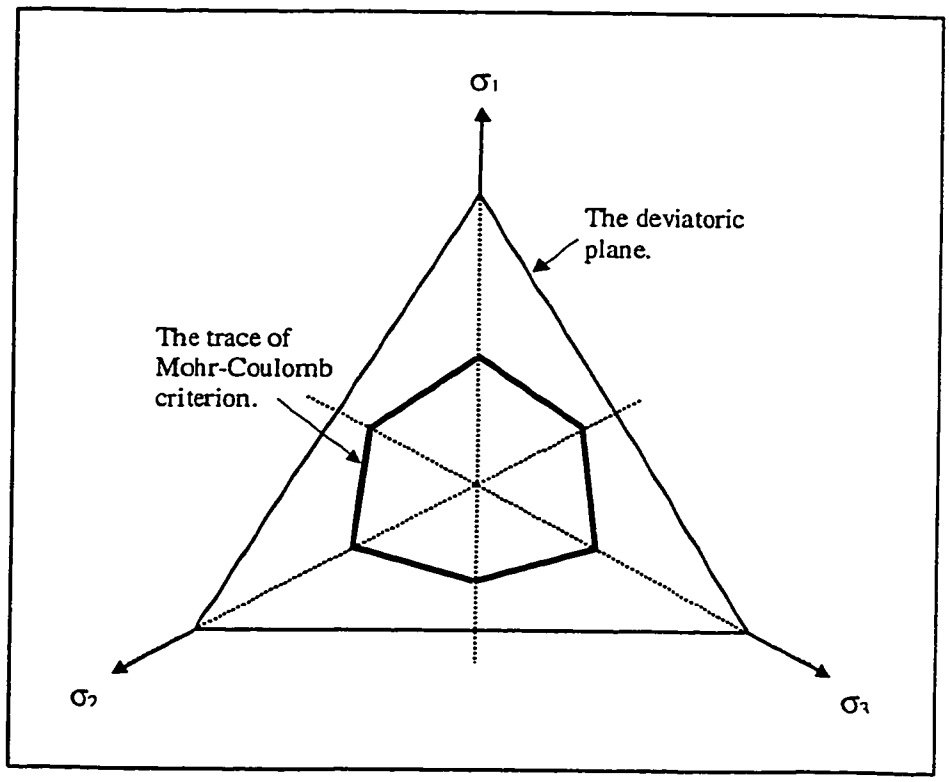

Figure (3-5) The trace of Mohr-Coulomb failure criterion on the deviatoric plane.

3.2.6 The Pile-Soil Interface Element

Since negative skin friction is a function of the relative movement between the pile and the soil, a slip element, therefore, was employed to simulate the interaction behavior at soil-pile interface. The slip element that was used in the analysis, similar to

the one proposed by Desai et al. (1984), was treated as one dimensional element with six distinct nodes; each three are in the longitudinal direction of the element, as shown in Figure (3-3, c). It is also formulated to behave as a linear elastic-perfect plastic Mohr-Coulomb material which is governed by the following parameters:

- the soil cohesion, c
- the interface angle, δ
- the stiffness in normal direction, $K_n = \frac{E(1-\nu)}{(1+\nu)(1-2\nu)}$,

  E = soil modulus of elasticity,

  ν = soil Poisson's ratio
- the shear modulus, $K_s = G$
- the residual shear modulus, K_{res} (usually $0.01K_s \geq K_{res} \geq 0.001K_s$),
- the element thickness, t (usually $0.1l_e > t > 0.01l_e$, where l_e = the element length).

According to the foregoing constitutive relationship, the slip element behaves elastically till the shear stress reaches the limiting shear stress defined by the Mohr-Coulomb equation,

$$\tau = c + \sigma_n \tan\delta \qquad \ldots\ldots \text{(3.4)}$$

If the shear stress exceeds the limiting shear stress, the shear modulus, K_s , is replaced by the residual shear modulus, K_{res} , because of which the relative slip between the soil and the pile is permitted.

Throughout this investigation, the following values were assigned to the parameters representing the material properties:

$c = 0$, since the soil is assumed normally consolidated clay

$\delta = 0.9\phi$, where ϕ = the shearing resistance angle of the surrounding soil

$K_{res} = 0.01G$, E = 10,000 kPa, $\nu = 0.2$,and t = 3 cm.

3.2.7 Types of Loading

Two types of loading were taken into account in the analysis. The first type is the surcharge loading, which acts on the ground level from the pile shaft to the end of the mesh, as shown in Figure (3-6). Different values of surcharging were used, and determined according to a dimensionless parameter N_s defined by the following relationship:

$$N_s = L\gamma'/S \qquad \ldots\ldots (3.5)$$

where L = pile length

γ' = effective unit weight of soil

S = surcharge pressure

N_s represents the ratio between the stress level at the pile tip and the surcharge pressure. The values assigned to N_s are: 5, 10, and 15.

The vertical load, which is the second loading type, was considered as an allowable load calculated as follows:

$$P_a = Q_u/FS \qquad \ldots\ldots (3.6)$$

where Q_a = the allowable vertical load on a single pile

Q_u = the ultimate vertical load on a single pile

FS = factor of safety

Three factors of safety, FS = 2, 4, and ∞ (i.e. no loading was applied on the pile) were used to determine each allowable load. The effective stress method (β - Method) was used to determine the ultimate load, Q_u, through the following relationship:

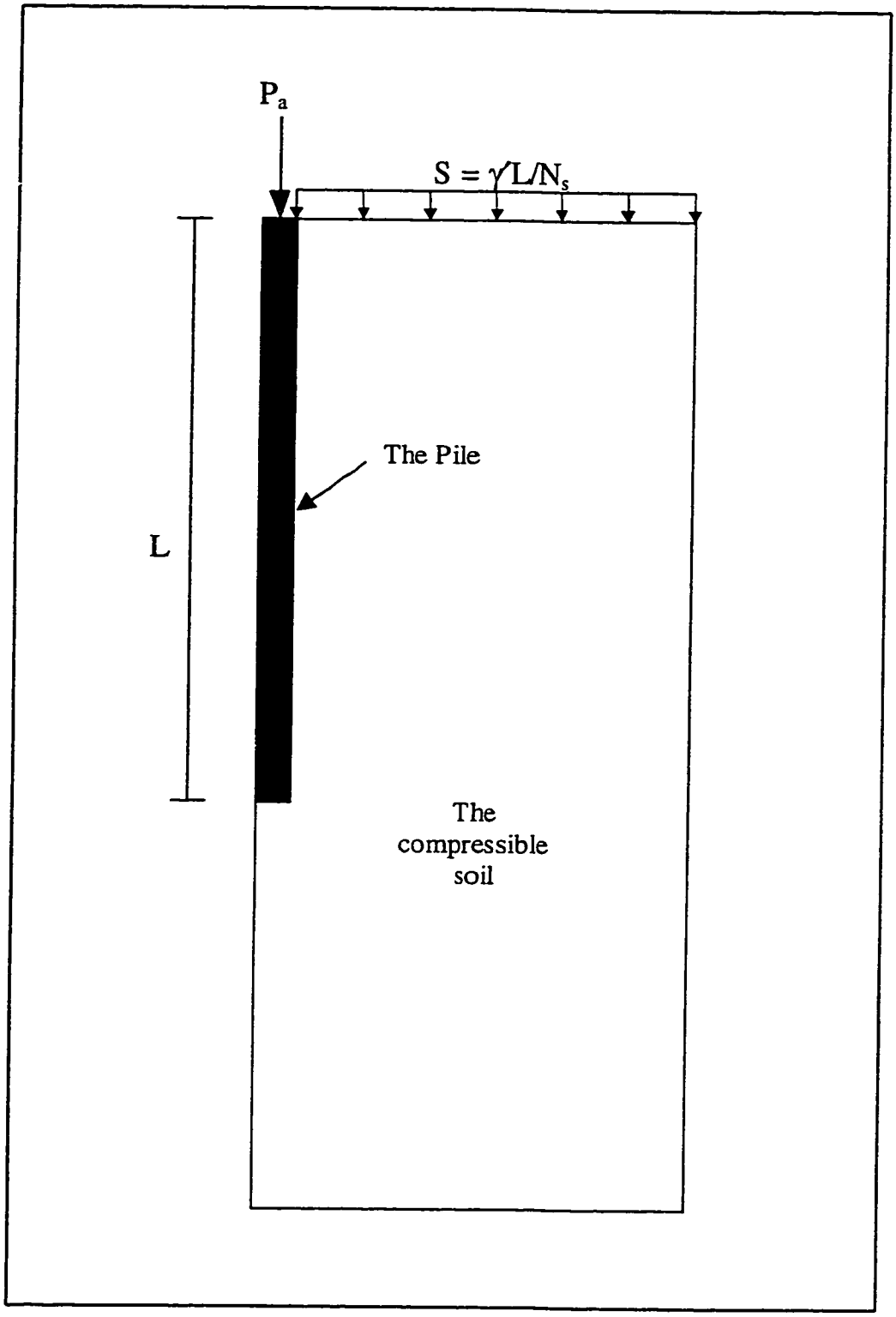

Figure (3-6) Types of loading applied on the pile and the soil

$$Q_u = \pi D \int_0^L K_o (\gamma' z) \tan\phi \, dz \qquad \ldots\ldots (3.7)$$

where D = the pile diameter

γ' = effective unit weight of soil

L = the pile length

ϕ = angle of shearing resistance

K_o = coefficient of earth pressure at rest, and can be approximated to

$$K_o = 1 - \sin\phi \qquad \ldots\ldots (3.8)$$

Integrating (3.7) will give

$$Q_u = \tfrac{1}{2} \pi D K_o (\gamma L^2) \tan\phi \qquad \ldots\ldots (3.9)$$

Equation (3.9) provides an approximate estimation of the ultimate capacity of a single pile. Further, it might overestimate the shaft capacity of long piles (L > 50 m). Nevertheless, it is only intended herein to emphasize the influence of the level of loading or the factor of safety on the location of the neutral depth. Thus equation (3.9) is believed to serve the need of this purpose.

Based on the information presented by Poulos and Davis (1972) that for soft soils local slippage between the pile and the soil cancels the effect of delayed pile installation specially if one-way drainage condition exists, hence no consideration of delayed installation of a pile was made throughout the study. In performing the analysis, therefore, the surcharge loading was applied first in five increments for duration of 10 minutes. Similarly, the vertical load was then applied in five increments for duration of 10 minutes. Finally, the soil was permitted to consolidate for a period of time, divided into twenty increments, sufficient to complete the consolidation process.

3.2.8 The program CRISP

The numerical model described in this work was carried out by the program CRISP (CRItical State Program) 1994 version. This program is a finite element code which was developed by the Cambridge Soil Mechanics Group. It is provided with the following main features:

(i) Types of analysis:

Undrained, drained and coupled consolidation analysis can be handled by the package either for two dimensional plane strain or axisymmetric, or three dimensional plain strain solid bodies.

(ii) Soil models:

The following models are available in CRISP 94:

(a) anisotropic linear elastic

(b) inhomogeneous linear elastic (properties vary linearly with depth)

(c) elastic-perfectly plastic with Von Mises, Tresca, Drccker-Peager, or Mohr-Coulomb yield criteria

(d) critical state soil models, both Cam-clay and modified Cam-clay models

(e) Schofield's three part yield surface soil model

(iii) Element types:

The program offers the following element types:

(a) linear strain bar element with quadratic shape function,

(b) two types of linear strain triangle elements with quadratic shape functions; one is for drained and undrained analyses, the other includes excess pore pressure unknowns at its vertex for consolidation analysis,

(c) two linear strain quadrilateral elements; the one for consolidation analysis is provided with linearly varying excess pore pressure,

(d) two cubic strain triangle elements; for consolidation purposes, one of the elements includes cubic variation of excess pore pressures,

(e) two linear strain brick elements; the one used for consolidation is provided with linearly varying excess pore pressures,

(f) linear strain beam element with quadratic displacement function,

(g) and, linear strain slip element with quadratic displacement function.

(iv) Boundary Conditions:

Element sides can be given prescribed incremental values of displacements or excess pore pressure. Loading could be applied as nodal loads or surface traction along the element edges. Automatic calculations of loads due to added or removed elements simulating the process of construction or excavation.

It is worth mentioning that the program uses a tangent stiffness solution scheme in which the global stiffness matrix is updated in each increment. For elastic-perfectly plastic models, the stress state is corrected back to the yield surface at each increment. Therefore, a limited increment size is required in order to achieve a reasonable convergence.

3.2.9 Variables Considered

Table (3.1) summarizes the range of the parameters that were considered in this study. The range of the internal friction angle (ϕ) that represents a normally consolidated clay was taken from Clayton et. al. (1986).

Table 3.1 Summary of the range of parameters used in the present investigation.

Angle of shearing resistance, ϕ (degrees)	18 to 30
Surcharging parameter, N_s	5 to 15
Factor of safety, FS	2 to 4, and ∞
slenderness ratio, L/D	25 to 100
Length of pile, L (m)	15 to 60

Because of their insensitivity to the location of the neutral depth, soil elastic parameters ν_s and E_s were excluded from the study. The ranges of the preliminary parameters are shown in Table (3.2). The shear stress distribution and the location of neutral depth are shown in Figures (3-7) through (3-9).

Table (3.2) Summary of the range used in the preliminary investigation of the effect of soil elastic parameters.

Elastic modulus of soil, E_s (kPa)	5,000 to 10,000
Poisson's ratio, ν_s	0.15 to 0.25

It was further noticed in the preliminary investigation that the change of the neutral point location during the consolidation process was infinitesimally small. Figures (3-10) to (3-12) show that the variation of neutral plane depth with time is negligible. This is consistent with the experimental data provided by Leung et al (1991).

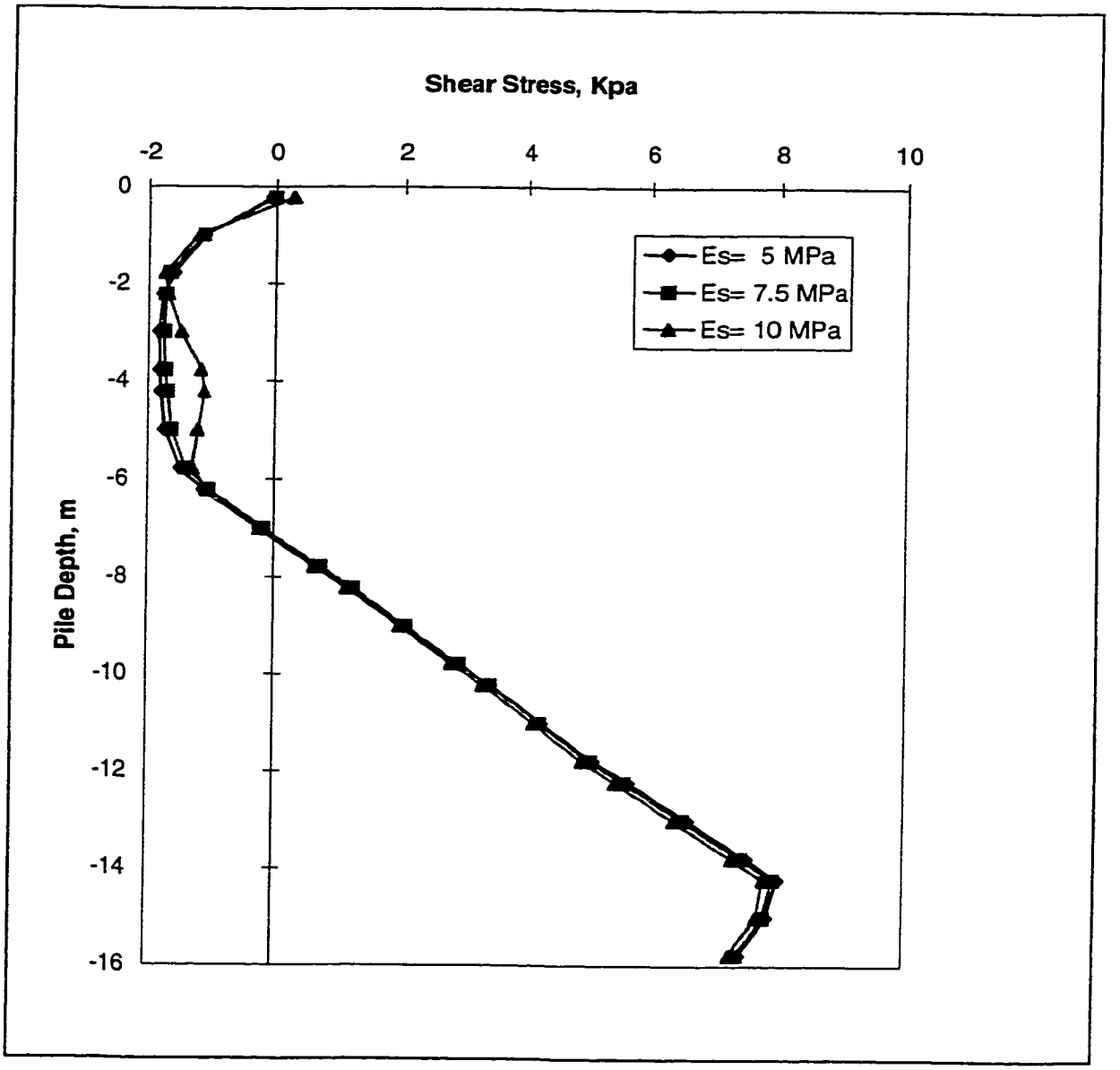

Figure (3-7) Shear stress distribution along pile length for different soil moduli of elasticity (Surcharge pressure = 5 kPa and $\nu = 0.15$)

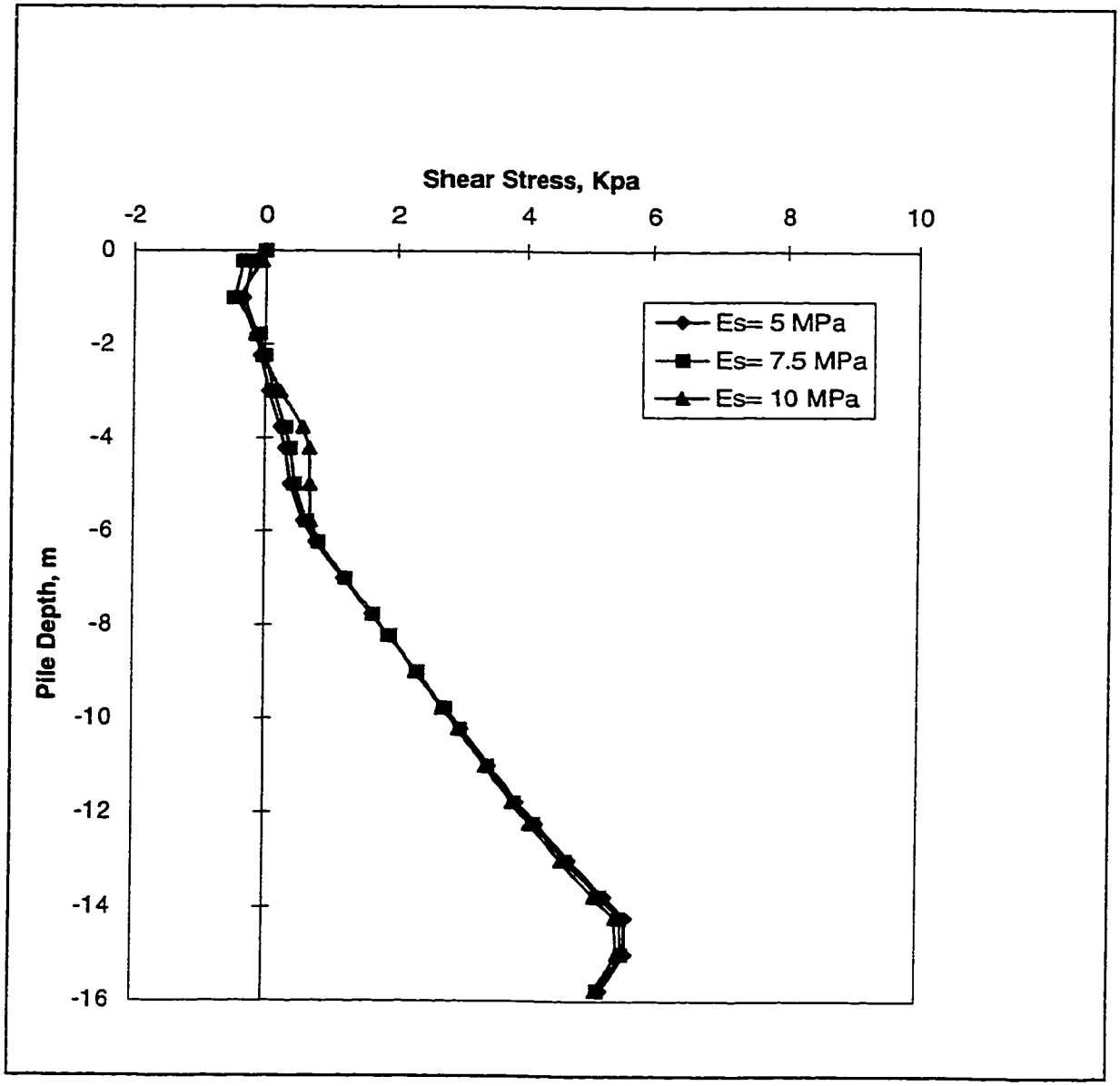

Figure (3-8) Shear stress distribution along pile length for different soil moduli of elasticity (Surcharge pressure = 10 kPa and $\nu = 0.2$)

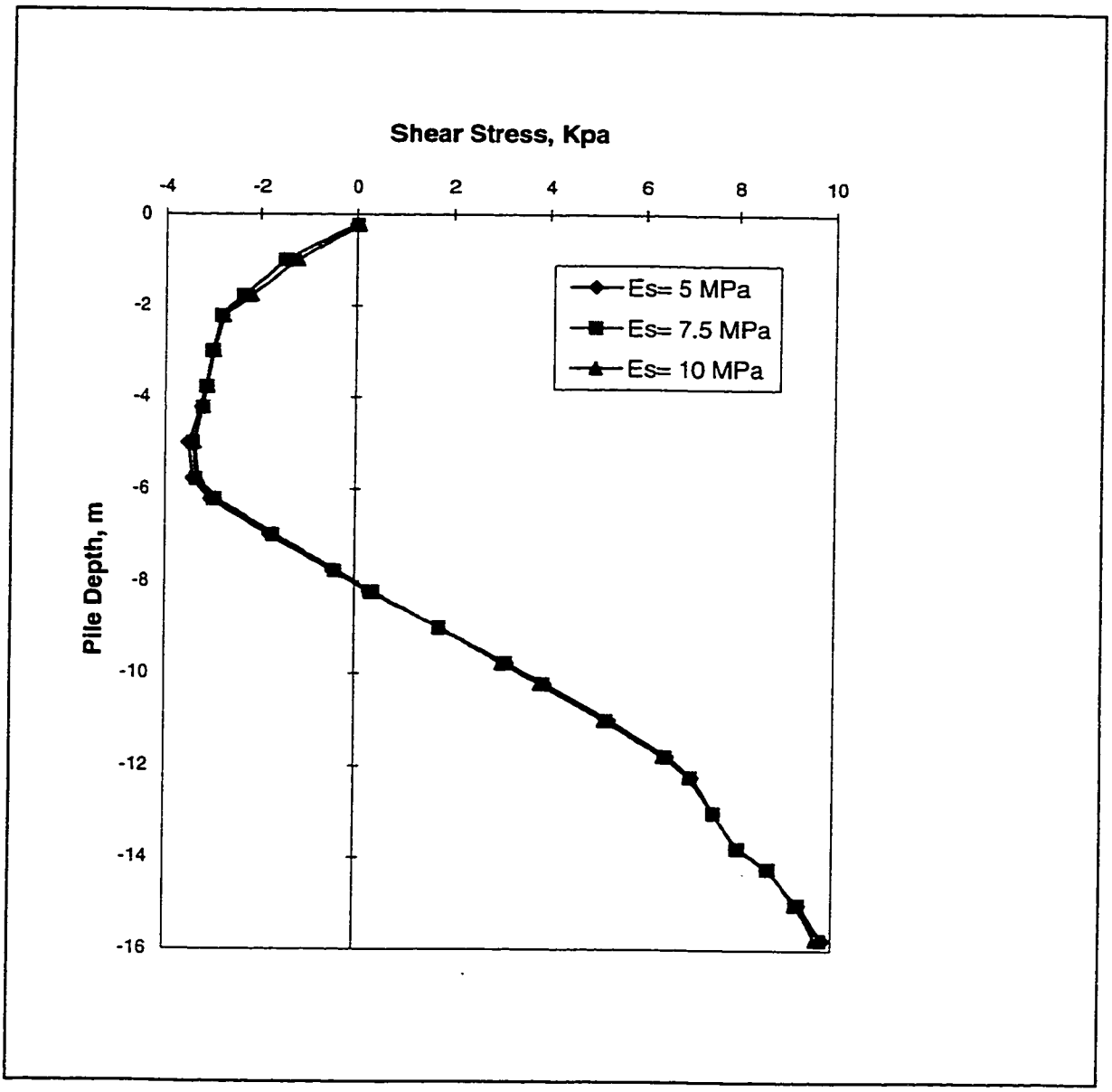

Figure (3-9) Shear stress distribution along pile length for different soil moduli of elasticity (Surcharge pressure = 15 kPa and $\nu = 0.25$)

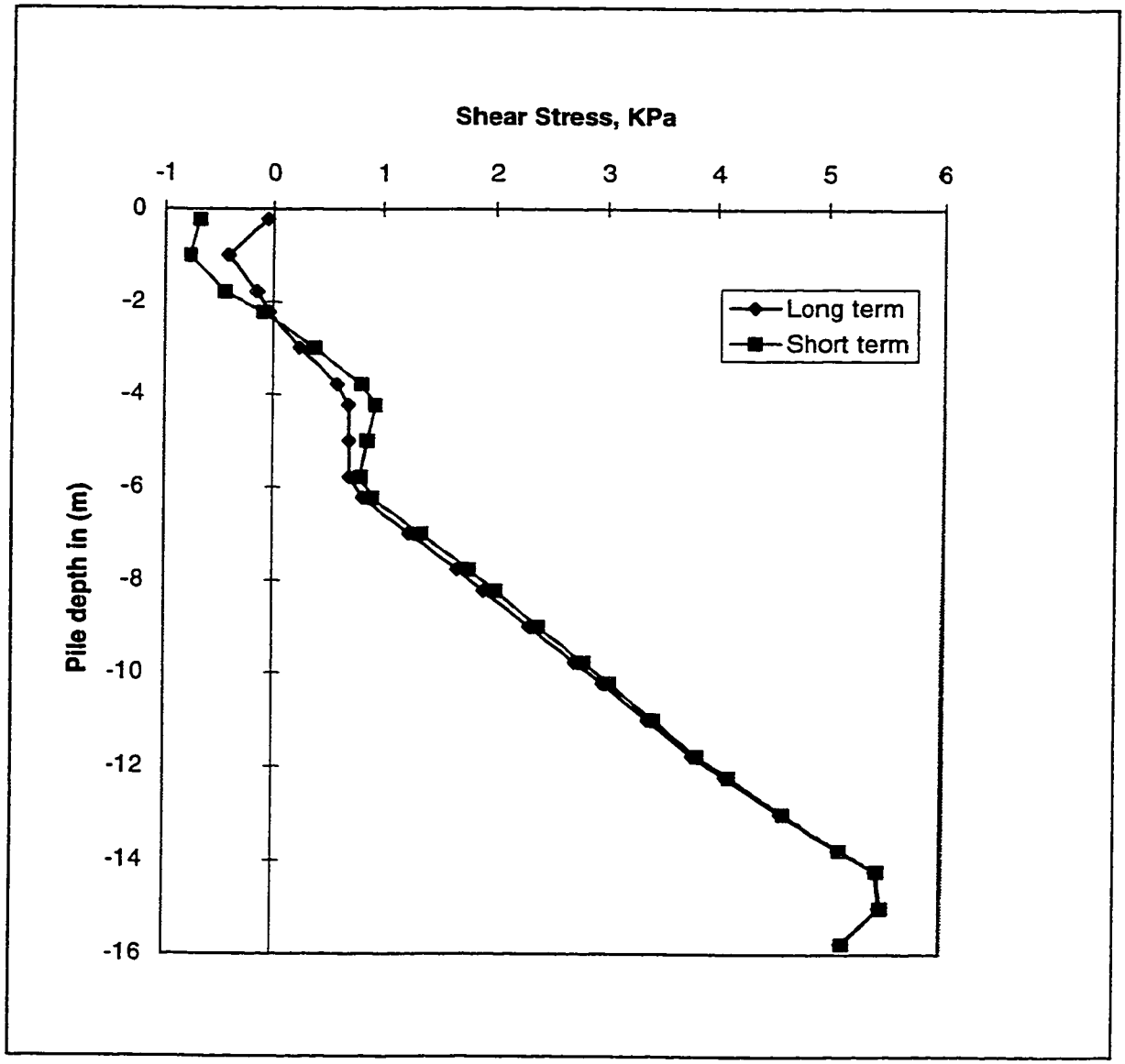

Figure (3-10) Long and short term distribution of skin friction along the pile length (Surcharge pressure = 5 kPa and ν = 0.15)

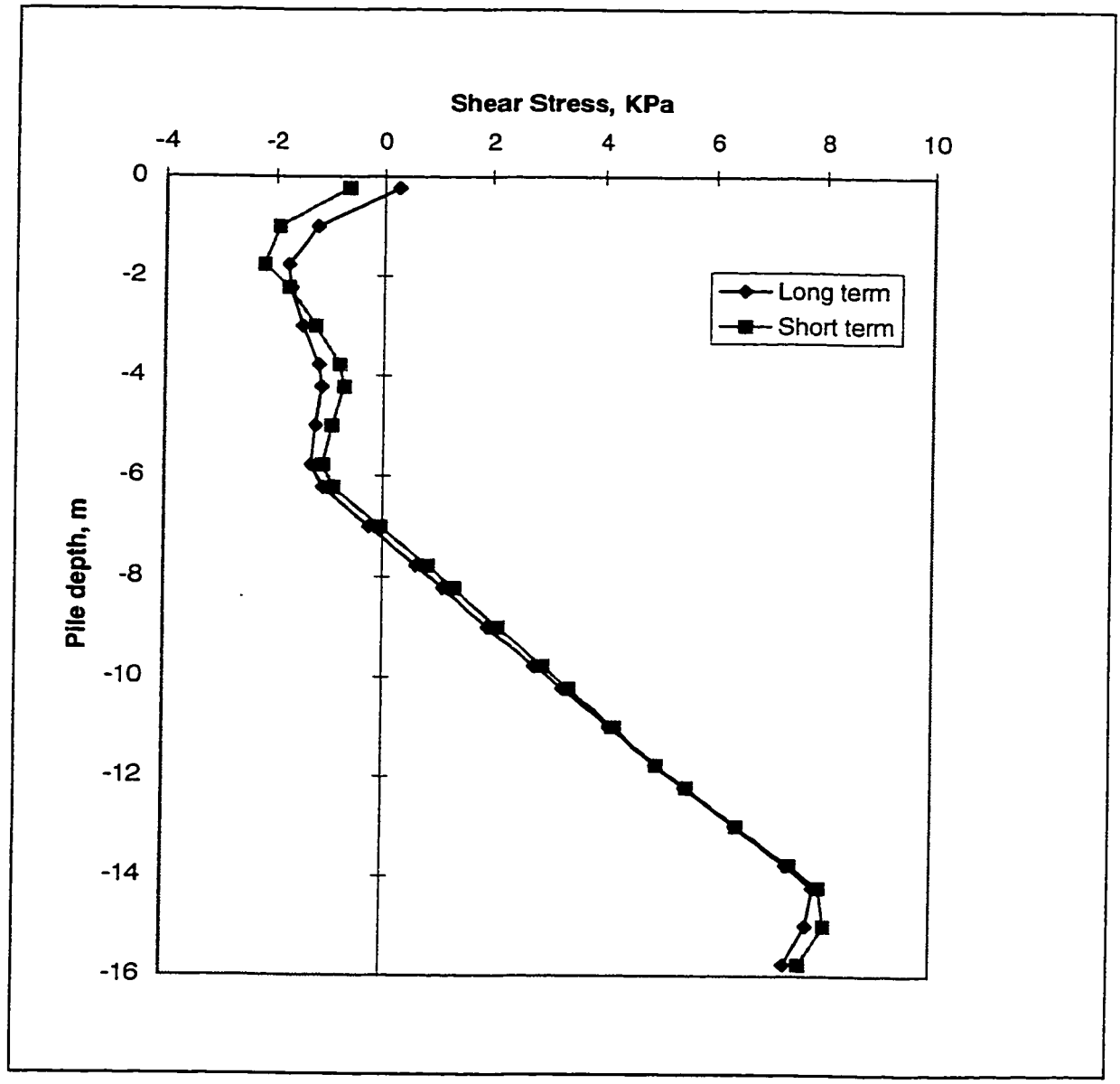

Figure (3-11) Long and short term distribution of skin friction along the pile length (Surcharge pressure = 10 kPa and $\nu = 0.20$)

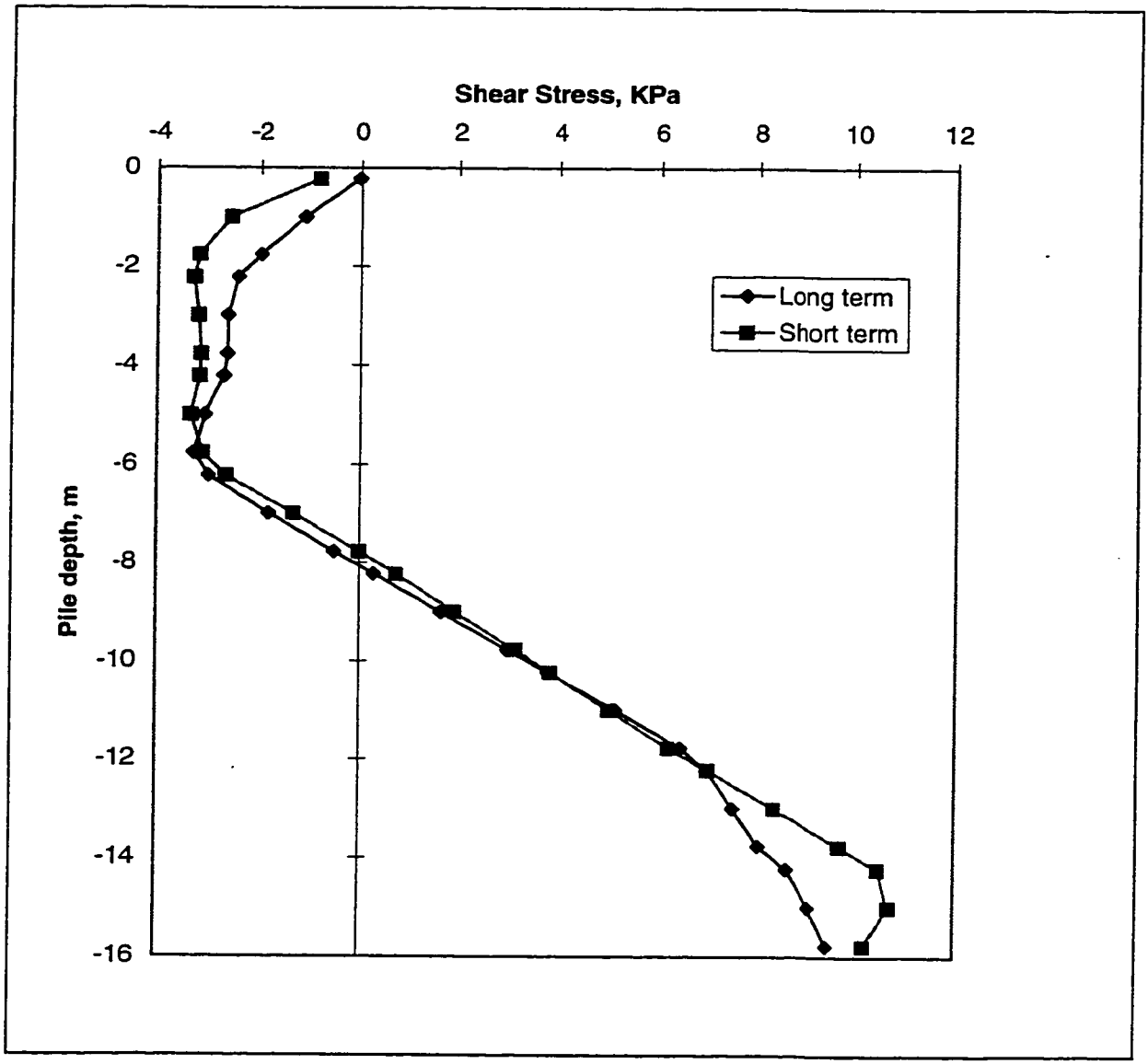

Figure (3-12) Long and short term distribution of skin friction along the pile length (Surcharge pressure = 15 kPa and ν = 0.25)

CHAPTER 4
RESULTS AND ANALYSIS

4.1 GENERAL

In this chapter details of the test procedure and a comparison with field data are given. Explanation of the test program and the numerical results of the finite element analysis involving both the axial load and the surcharge load are presented. The factors affecting the location of the neutral plane are examined by means of a parametric study. Furthermore, a design approach including a design formula and design procedure are presented.

4.2 TEST PROCEDURE

The test procedure will be demonstrated by considering a floating pile embedded in a homogeneous saturated clay with an angle of shearing resistance,ϕ = 26 °. The pile dimensions are 15 m. in length and 0.3 m. in diameter, and the surcharge pressure, S, applied on the surrounding soil is equal to 12 kPa.

First, the mesh size should be determined according to the given pile dimensions. Therefore, from section 3.2.1, the width of the mesh, W, is equal to the bigger of r + 0.6L or r + 25D, where r is the pile radius. Thus, W = 0.15 + 0.6(15) = 9.15 m (since 0.6(15) > 25(0.3)). Similarly, the mesh height, B, is equal to 1.7L. Hence, B = 1.7(15) = 25.5 m. Figure (3-2) provides the necessary information needed to subdivide and distribute the finite elements in the mesh.

Then, the applied axial load are computed by determining the ultimate capacity of the pile from equation (3.9), thus Qu = 230 kN, and the allowable (axial) loads corresponding to factors of safety, FS = 2 and 4 are P_{a1}= 115 KN and P_{a2} = 57.5 kN respectively. The surcharge factor, Ns, can be calculated from equation (3.5). Hence, for S = 12, Ns = 10.

Finally, performing the analysis by dividing it into 30 increments. These increments are grouped into three increment blocks. The first block, which represents the axial load applied on the pile, is divided into five increments of two minutes in each so no consolidation will take place during loading. For the same reason, the surcharge pressure is applied in the second block and divided into five increments of two minutes in each. The third block is divided into 20 increments of equal duration to allow for consolidation. The total duration of this block is ten years in which the consolidation process is believed to be completed. The consolidation considered herein is of single drainage that takes place at the ground level.

The summary of the input data of the pile, the soil, and the interface element required for the analysis are presented in the tables shown below. The result of this test is shown in Figure (4-1). It shows the skin friction distribution along the pile and the location of the neutral plane for three different loading conditions.

Table (4.1) The pile input data

Length, L (m)	Diameter, D (m)	Modulus of Elasticity, E_p (GPa)	Poisson's Ratio, ν_p	Shear Modulus, G (GPa)	Unit Weight, γ_c (kN/m^3)
15	0.3	20	0.33	7.5	23

Table (4.2) The soil input data

Modulus of Elasticity, E_s (kPa)	Poisson's Ratio, ν_s	Shear Modulus, G_s (kPa)	The Angle of Shearing Resistance, ϕ	Submerged Unit Weight, γ' (kN/m^3)	Coefficient of Permeability, k_x & k_y (m/s)
10,000	0.2	4	26	8	1.0×10^{-7}

Table (4.3) The interface element input data

The Interface Angle of Shearing Resistance, δ	The Stiffness of Normal Direction, K_n (kPa)	Shear Modulus, G (kPa)	Residual Shear Modulus, K_{res} (kPa)	Thick-ness, t (cm)
23.4	11,100	4,160	41.6	3

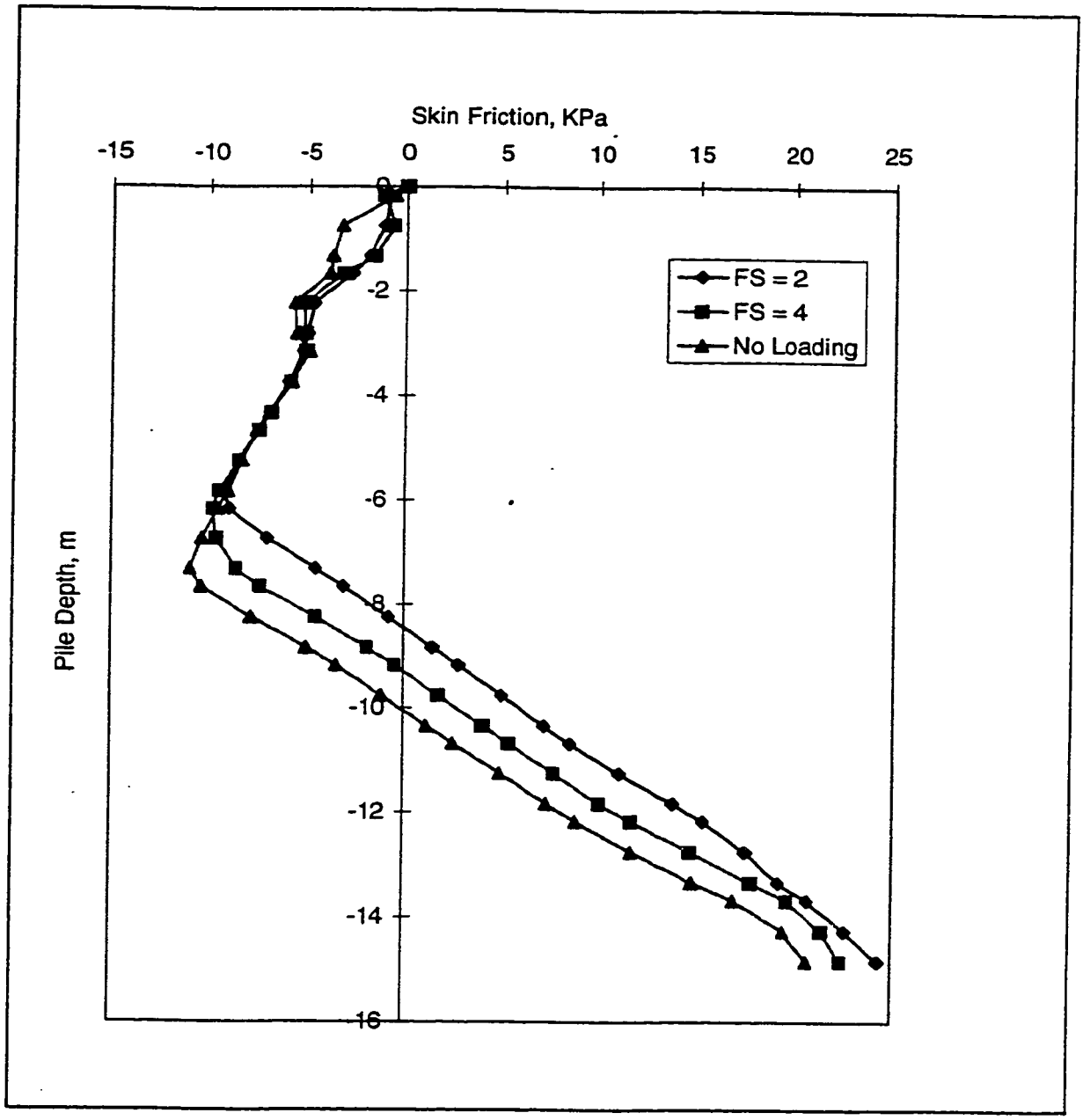

Figure (4-1) Skin friction distribution along the pile for different axial loads

4.3 COMPARISON WITH FIELD DATA

Indraratna et al. (1992) reported a field study of negative skin friction on a driven pile. The pile was a hollow prestressed concrete of 27 m. in length and 0.4 external diameter. The equivalent elastic modulus of the pile is determined to be 29.4 GPa. The pile was driven through fill and soft clay into a stiff clay stratum. The surrounding soil was loaded by an embankment of 2 m. in height to induce negative skin friction on the pile. Piezometer readings indicated that the primary consolidation was completed after 265 days of placing the embankment.

The input data representing the pile material and the pile-soil interface elements used in the comparison was taken from those reported by Indraratna et al. The soil strength parameters, however, were extracted from the information provided for the interface elements. Tables (4.4) to (4.5) summarize the input data used in the comparison for the soil, the pile, and the interface elements.

Table (4.4) The soil input properties

Depth (m)	E_s (MPa)	ν_s	G_s (MPa)	γ_t (kN/m^3)	c' (kPa)	ϕ	k_x, k_y (m/s)
-2 to 4	4.9	0.2	2.0	16.8	3	26	7.8×10^{-4}
4 to 10	4.9	0.2	2.0	16.8	5.9	25	6.4×10^{-5}
10 to 20	4.9	0.2	2.0	16.8	14.7	25	3.0×10^{-5}
20 to 24	6.37	0.2	2.65	16.8	5.9	23	4.3×10^{-5}
24 to 28	27.44	0.33	10.3	16.8	-	-	4.3×10^{-5}

Table (4.5) The pile input data

L (m)	D (m)	E_p (GPa)	ν_p	G (GPa)	γ_c (kN/m^3)
27	0.4	29.4	0.33	11.0	24.5

Table (4.6) The interface elements input data

Depth (m)	c′ (kPa)	δ	K_n (kPa)	G (kPa)	K_{res} (kPa)	t (cm)
-2 to 20	6	20	5450	2000	20	3
20 to 24	6	23	9440	2650	26.5	3

Figure (4-2) shows that the computed and measured negative skin friction distribution along the pile are in good agreement. The difference in the location of the neutral plane of the two curves is about 1.1 m. In terms of normalized neutral plane depth, L_{NP}/L, the computed one showed a value of (0.69), whereas the measured value is about (0.73). Thus, the difference in the two values is appreciably small.

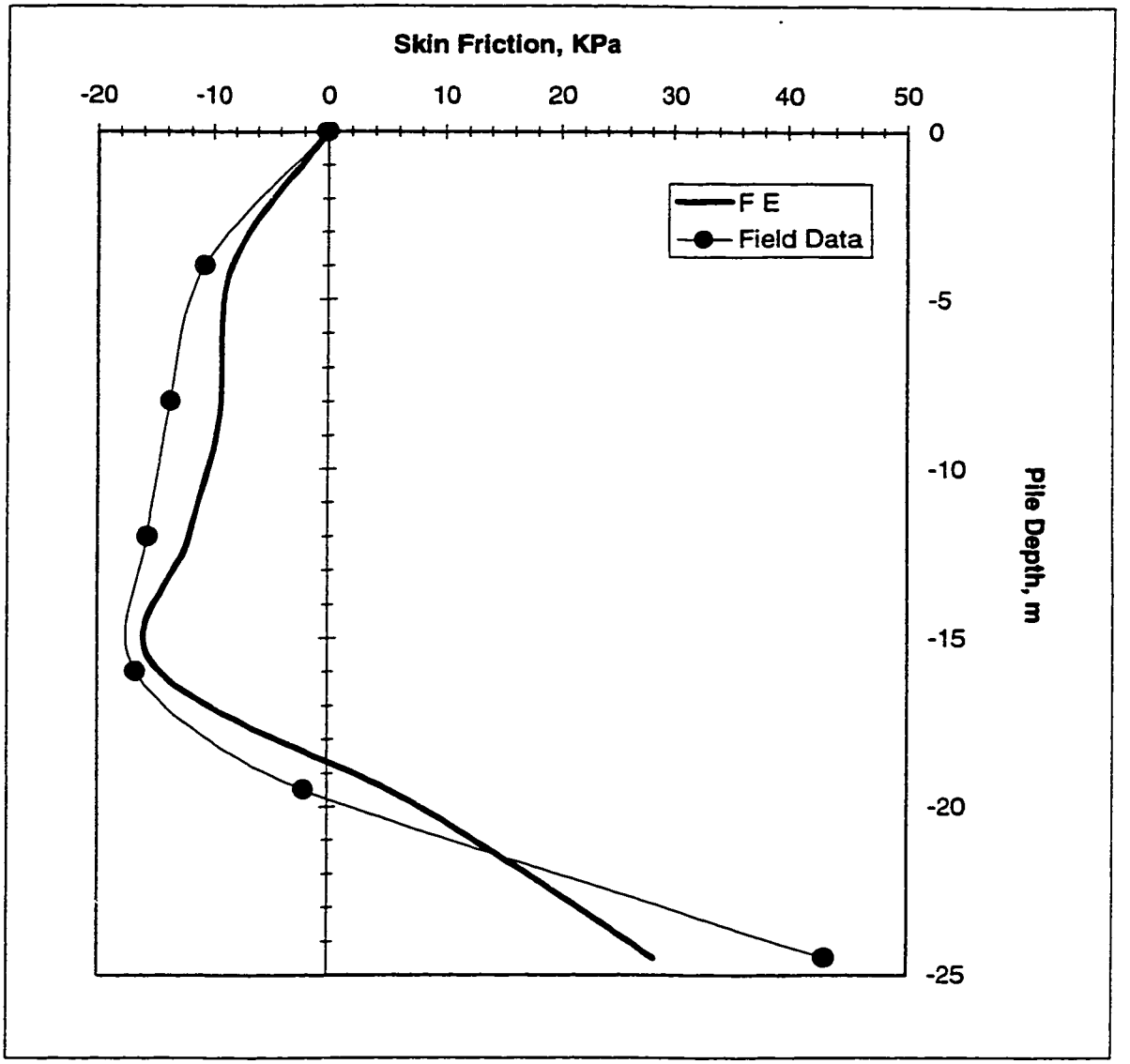

Figure (4-2) The comparison between the field data and numerical analysis

4.4 TEST PROGRAM AND RESULTS

From the literature survey conducted in chapter 2, a general understanding of the nature of negative skin friction has been gained. Thus, number of factors were believed to have influences on the depth of neutral plane, which can summarized in the following:

(a) the pile length, L, and diameter, D,

(b) the surcharge pressure, S,

(c) the magnitude of the axial load, P_a, applied on the pile head, and

(d) the strength (ϕ) and deformation (E_s, ν_s) properties of the surrounding soil.

To preserve generality, the above factors were normalized to give the following dimensionless ratios:

(a) The slenderness ratio, L/D, represents the pile dimensions.

(b) The surcharge factor, $Ns = \gamma L/S$, besides its representation to the surcharge pressure, emphasizes the effect of the pile length and the associated increase in the overburden pressure at the pile tip level.

(c) The factor of safety, $FS = Q_u/P_a$, represents the level of loading applied on the pile head.

Since the soil strength parameter, ϕ, represents the angle of shearing resistance, it requires no normalization. For the reasons mentioned in section 3.2.9, the soil deformation properties (E_s, ν_s) were excluded from the study.

The parametric study presented in this chapter is based on 432 trial analysis employing the numerical model developed in chapter 3. The input data and its results are listed and divided into 3 major groups of different values of factor of safeties. Each group consists of four sub-groups of different angles of shearing resistance. Each sub-group is divided into four series of slenderness ratios, where the influence of each parameter is isolated and examined individually, as presented in Tables (4.1) to (4.12).

Table (4.7) Test Results for Group I-1, FS =2 and ϕ = 18

Test No.	Series No.	Pile Length (m)	Ns	L/D	Neutral Depth (m)
1	1	15	5	25	8.86
2				50	8.68
3				75	8.63
4				100	8.64
5			10	25	8.17
6				50	8.68
7				75	8.90
8				100	9.04
9			15	25	7.43
10				50	8.21
11				75	8.43
12				100	8.79
13	2	30	5	25	17.56
14				50	17.43
15				75	17.35
16				100	17.57
17			10	25	16.12
18				50	17.04
19				75	17.12
20				100	17.57
21			15	25	14.33
22				50	15.96
23				75	16.56
24				100	16.78

Test No.	Series No.	Pile Length (m)	Ns	L/D	Neutral Depth (m)
25	3	45	5	25	26.34
26				50	26.38
27				75	26.34
28				100	26.39
29			10	25	23.98
30				50	25.01
31				75	25.78
32				100	25.91
33			15	25	21.35
34				50	23.69
35				75	24.47
36				100	24.97
37	4	60	5	25	34.82
38				50	34.92
39				75	34.78
40				100	34.79
41			10	25	31.68
42				50	33.46
43				75	33.78
44				100	34.33
45			15	25	28.35
46				50	31.31
47				75	32.20
48				100	33.18

Table (4.8) Test Results for Group I-2, FS =2 and $\phi = 22$

Test No.	Series No.	Pile Length (m)	Ns	L/D	Neutral Depth (m)
49	5	15	5	25	8.84
50				50	8.73
51				75	8.72
52				100	8.72
53			10	25	7.97
54				50	8.57
55				75	8.82
56				100	8.97
57			15	25	7.05
58				50	8.01
59				75	8.26
60				100	8.50
61	6	30	5	25	17.59
62				50	17.36
63				75	17.31
64				100	17.20
65			10	25	15.77
66				50	16.82
67				75	17.09
68				100	17.51
69			15	25	13.75
70				50	15.48
71				75	16.29
72				100	16.47

Test No.	Series No.	Pile Length (m)	Ns	L/D	Neutral Depth (m)
73	7	45	5	25	26.24
74				50	26.14
75				75	26.21
76				100	26.50
77			10	25	23.44
78				50	25.03
79				75	25.41
80				100	25.64
81			15	25	20.49
82				50	22.83
83				75	23.86
84				100	24.40
85	8	60	5	25	35.17
86				50	34.60
87				75	35.21
88				100	35.41
89			10	25	31.18
90				50	33.26
91				75	33.20
92				100	33.67
93			15	25	29.87
94				50	30.61
95				75	31.93
96				100	32.22

Table (4.9) Test Results for Group I-3, FS =2 and $\phi = 26$

Test No.	Series No.	Pile Length (m)	Ns	L/D	Neutral Depth (m)
97	9	15	5	25	8.78
98				50	8.56
99				75	8.63
100				100	8.86
101			10	25	7.86
102				50	8.49
103				75	8.75
104				100	8.94
105			15	25	6.78
106				50	7.84
107				75	8.04
108				100	8.27
109	10	30	5	25	17.64
110				50	17.50
111				75	17.36
112				100	17.44
113			10	25	15.48
114				50	16.74
115				75	17.23
116				100	17.46
117			15	25	13.32
118				50	15.34
119				75	16.02
120				100	16.32

Test No.	Series No.	Pile Length (m)	Ns	L/D	Neutral Depth (m)
121	11	45	5	25	26.34
122				50	26.30
123				75	26.43
124				100	26.11
125			10	25	23.09
126				50	24.89
127				75	25.77
128				100	26.07
129			15	25	19.78
130				50	22.75
131				75	23.84
132				100	24.36
133	12	60	5	25	34.61
134				50	34.69
135				75	34.08
136				100	34.86
137			10	25	30.62
138				50	33.18
139				75	33.96
140				100	34.18
141			15	25	26.34
142				50	30.13
143				75	31.68
144				100	32.12

Table (4.10) Test Results for Group I-4, FS =2 and ϕ =30

Test No.	Series No.	Pile Length (m)	Ns	L/D	Neutral Depth (m)
145	13	15	5	25	8.75
146				50	8.75
147				75	8.68
148				100	8.80
149			10	25	7.76
150				50	8.39
151				75	8.70
152				100	8.84
153			15	25	6.62
154				50	7.63
155				75	8.00
156				100	8.12
157	14	30	5	25	17.51
158				50	17.49
159				75	17.42
160				100	17.36
161			10	25	15.33
162				50	16.66
163				75	17.08
164				100	17.40
165			15	25	13.07
166				50	15.09
167				75	15.88
168				100	16.08

Test No.	Series No.	Pile Length (m)	Ns	L/D	Neutral Depth (m)
169	15	45	5	25	25.95
170				50	26.18
171				75	26.21
172				100	25.92
173			10	25	22.81
174				50	24.64
175				75	25.60
176				100	25.59
177			15	25	19.36
178				50	22.48
179				75	23.62
180				100	23.73
181	16	60	5	25	34.38
182				50	34.26
183				75	34.11
184				100	34.06
185			10	25	30.14
186				50	32.37
187				75	33.51
188				100	33.34
189			15	25	25.64
190				50	29.76
191				75	31.32
192				100	31.91

Table (4.11) Test Results for Group II-1, FS =4 and ϕ =18

Test No.	Series No.	Pile Length (m)	Ns	L/D	Neutral Depth (m)
193	17	15	5	25	9.54
194				50	9.27
195				75	9.23
196				100	9.26
197			10	25	9.26
198				50	9.46
199				75	9.54
200				100	9.67
201			15	25	8.63
202				50	9.14
203				75	9.32
204				100	9.56
205	18	30	5	25	19.27
206				50	18.63
207				75	18.37
208				100	18.35
209			10	25	18.39
210				50	18.91
211				75	19.06
212				100	19.19
213			15	25	17.09
214				50	18.22
215				75	18.77
216				100	18.92

Test No.	Series No.	Pile Length (m)	Ns	L/D	Neutral Depth (m)
217	19	45	5	25	28.97
218				50	28.26
219				75	28.29
220				100	28.38
221			10	25	27.54
222				50	28.26
223				75	28.41
224				100	28.82
225			15	25	25.63
226				50	27.41
227				75	28.15
228				100	28.48
229	20	60	5	25	38.72
230				50	37.68
231				75	37.56
232				100	38.39
233			10	25	36.73
234				50	37.76
235				75	38.21
236				100	38.00
237			15	25	34.06
238				50	36.05
239				75	37.34
240				100	37.59

Table (4.12) Test Results for Group II-2, FS = 4 and $\phi = 22$

Test No.	Series No.	Pile Length (m)	Ns	L/D	Neutral Depth (m)
241	21	15	5	25	9.54
242				50	9.28
243				75	9.20
244				100	9.27
245			10	25	9.09
246				50	9.39
247				75	9.57
248				100	9.66
249			15	25	8.36
250				50	8.94
251				75	9.19
252				100	9.30
253	22	30	5	25	19.24
254				50	18.54
255				75	18.44
256				100	18.45
257			10	25	18.14
258				50	18.72
259				75	18.98
260				100	19.20
261			15	25	16.60
262				50	17.88
263				75	18.43
264				100	18.70

Test No.	Series No.	Pile Length (m)	Ns	L/D	Neutral Depth (m)
265	23	45	5	25	29.00
266				50	28.13
267				75	28.28
268				100	28.10
269			10	25	27.07
270				50	28.06
271				75	28.48
272				100	28.62
273			15	25	24.85
274				50	26.80
275				75	27.67
276				100	28.04
277	24	60	5	25	38.40
278				50	36.95
279				75	37.12
280				100	37.51
281			10	25	36.04
282				50	36.97
283				75	37.80
284				100	38.40
285			15	25	35.58
286				50	35.63
287				75	36.93
288				100	37.37

Table (4.13) Test Results for Group II-3, FS = 4 and ϕ =26

Test No.	Series No.	Pile Length (m)	Ns	L/D	Neutral Depth (m)
289	25	15	5	25	9.54
290				50	9.38
291				75	9.28
292				100	9.33
293			10	25	8.96
294				50	9.29
295				75	9.47
296				100	9.59
297			15	25	8.18
298				50	8.78
299				75	9.04
300				100	9.15
301	26	30	5	25	19.10
302				50	18.79
303				75	18.68
304				100	18.60
305			10	25	17.77
306				50	18.56
307				75	18.93
308				100	19.09
309			15	25	16.23
310				50	17.63
311				75	18.17
312				100	18.46

Test No.	Series No.	Pile Length (m)	Ns	L/D	Neutral Depth (m)
313	17	45	5	25	28.56
314				50	28.52
315				75	28.14
316				100	28.22
317			10	25	26.70
318				50	27.72
319				75	28.39
320				100	28.54
321			15	25	24.27
322				50	26.36
323				75	27.27
324				100	27.73
325	28	60	5	25	37.72
326				50	37.47
327				75	37.91
328				100	37.32
329			10	25	35.59
330				50	36.99
331				75	37.70
332				100	37.95
333			15	25	32.33
334				50	35.12
335				75	36.23
336				100	36.94

Table (4.14) Test Results for Group II-4, FS =4 and ϕ =30

Test No.	Series No.	Pile Length (m)	Ns	L/D	Neutral Depth (m)
337	29	15	5	25	9.48
338				50	9.30
339				75	9.25
340				100	9.36
341			10	25	8.81
342				50	9.20
343				75	9.42
344				100	9.54
345			15	25	8.03
346				50	8.69
347				75	8.93
348				100	9.04
349	30	30	5	25	19.07
350				50	18.94
351				75	18.56
352				100	18.57
353			10	25	17.60
354				50	18.51
355				75	18.78
356				100	18.96
357			15	25	15.89
358				50	17.41
359				75	18.01
360				100	18.27

Test No.	Series No.	Pile Length (m)	Ns	L/D	Neutral Depth (m)
361	31	45	5	25	28.63
362				50	28.66
363				75	28.53
364				100	28.09
365			10	25	26.19
366				50	27.42
367				75	28.04
368				100	28.51
369			15	25	23.91
370				50	26.16
371				75	27.06
372				100	27.54
373	32	60	5	25	37.68
374				50	37.53
375				75	36.94
376				100	37.01
377			10	25	35.00
378				50	36.77
379				75	37.47
380				100	37.90
381			15	25	31.79
382				50	34.79
383				75	36.01
384				100	36.52

Table (4.15) Test Results for Group III-1, FS= ∞ and ϕ=18

Test No.	Series No.	Pile Length (m)	Ns	L/D	Neutral Depth (m)
385	33	45	5	25	31.50
386				50	30.45
387				75	30.17
388				100	30.03
389			10	25	30.88
390				50	31.38
391				75	31.23
392				100	31.38
393			15	25	29.69
394				50	30.72
395				75	31.27
396				100	31.49

Table (4.16) Test Results for Group III-2, FS= ∞ and ϕ=22

Test No.	Series No.	Pile Length (m)	Ns	L/D	Neutral Depth (m)
397	34	45	5	25	31.56
398				50	30.56
399				75	30.22
400				100	29.89
401			10	25	30.49
402				50	31.13
403				75	31.29
404				100	31.21
405			15	25	29.18
406				50	30.41
407				75	30.76
408				100	31.03

Table (4.17) Test Results for Group III-3, FS= ∞ and ϕ=26

Test No.	Series No.	Pile Length (m)	Ns	L/D	Neutral Depth (m)
409	35	45	5	25	31.26
410				50	30.50
411				75	30.19
412				100	30.00
413			10	25	30.06
414				50	30.87
415				75	31.17
416				100	31.10
417			15	25	28.66
418				50	29.90
419				75	30.55
420				100	30.69

Table (4.18) Test Results for Group III-4, FS= ∞ and ϕ=30

Test No.	Series No.	Pile Length (m)	Ns	L/D	Neutral Depth (m)
421	36	45	5	25	30.75
422				50	30.20
423				75	30.02
424				100	29.78
425			10	25	29.80
426				50	30.28
427				75	30.83
428				100	30.66
429			15	25	28.36
430				50	29.70
431				75	30.14
432				100	30.30

4.5 PARAMETRIC STUDY

4.5.1 The Effect of the angle of the shearing resistance (ϕ):

The effect of the angle of shearing resistance is illustrated by a graphical form in Figures (4-3) to (4-5). Each of the three Figures represents the tabulated values of the test results for Group I, Group II, and Group III, respectively. Figure (4-3) shows that the angle of shearing resistance has no considerable effect on the location of the neutral plane. It shows that the neutral plane depth reduces very slightly with the increased value of the angle of shearing resistance. It further can be noticed that this effect become more insignificant as the pile slenderness ratio, L/D, increases and the surcharge factor, Ns, decreases. Similarly, these remarks can also be seen in Figures (4-4) and (4-5).

The insignificant effect of the angle of shearing resistance can be attributed to the following two reasons. First, the low range in value of the angle of shearing resistance ($18< \phi < 30$) used in the analysis, although consistent with those for normally consolidated clay. Second, the constitutive model (linearly elastic-rigid plastic) used to represent the soil behavior. In the upper zone of the pile, due to the low overburden effective pressure and excessive settlement, the pile-soil interface reaches yielding regardless of the value of the angle of shearing resistance.

Because it has no influence on the neutral plane, the angle of shearing resistance will be excluded from any consideration in the proceeding parametric study.

4.5.2 The effect of the pile length to the pile diameter ratio (L/D):

The data of the test results was used to study the influence of L/D on the location of neutral plane. The variation of the normalized depth of neutral plane, L_{NP}/L, versus L/D for each value of the factor of safety, FS, and the surcharge factor, Ns, is presented in Figure (4-6). It can be seen from this figure that the variation of L_{NP}/L shows a gradual increase until L/D = 50, after which no significant increase is noticed. It is worth pointing out, however, that the variation of L_{NP}/L reaches its peak when the axial load is at its maximum and the surcharge pressure is at its minimum.

The explanation of the effect of L/D on the neutral plane is due to the compressibility of the pile material and the pile length. When negative skin friction is induced in a short pile, most of the downdrag is transmitted to the pile tip in form of penetration to the bearing layer. Whereas, for a long pile, the downdrag is mainly taken by the pile compressibility, and very little is transmitted to the tip. Thus, it can be said that the long pile performs in a general sense as an end bearing one.

Generally, L/D considered to be of a minor effect on the location of neutral plane, and its effect could be ignored for L/D > 50.

4.5.3 The effect of the surcharge factor (Ns):

The effect of Ns on L_{NP}/L, for different values of L/D and FS, is illustrated in Figure (4-7). It can be observed, from Figure (4-7), that Ns is inversely proportional to the depth of neutral plane. It is further noticed that the effect of surcharge pressure becomes more pronounced in short piles subjected to low axial loads. This is attributed to

the accelerated consolidation caused by the intensity of the surcharge pressure. An increase in the consolidation process will consequently increase the soil settlement, and thereby the relative movement between the pile and the soil increases in favor of the soil direction. This will shift the neutral plane to a deeper location.

4.5.4 The effect of the factor of safety (FS):

The variation of L_{NP}/L versus FS for each value of Ns and L/D is presented in Figure (4-8). This figure shows that the depth of neutral plane varies considerably with the increase of factor of safety, especially for FS $\leq$ 4. Whereas, the variation of L_{NP}/L drops significantly for FS > 4.

This can be explained by the fact that the neutral depth is governed by the relative displacement between the pile and the surrounding soil. In other words, when the relative displacement increases, in favor of the soil movement, the depth of neutral plane moves downward, and vice versa. Therefore, if the level of loading applied on the pile is high (say FS=2) the pile settlement will increase due to the accelerated consolidation process, and consequently the relative displacement will reduce. This fact was also observed indirectly from field experiments conducted by researchers such as Fellenius (1972) and Bozozuk (1980).

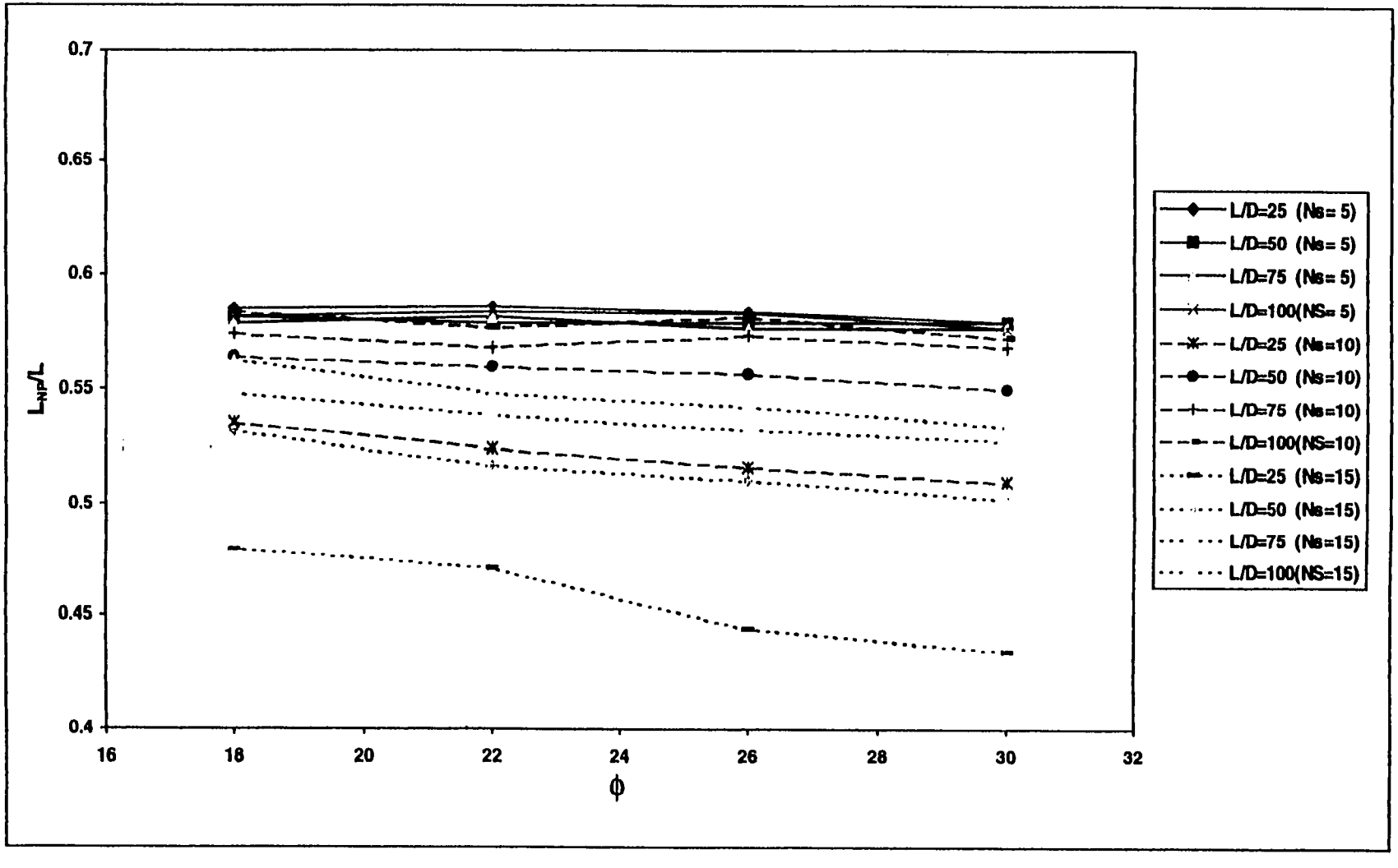

Figure (4-3) The effect of the soil shearing resistance, ϕ, on the location of the neutral plane for FS = 2

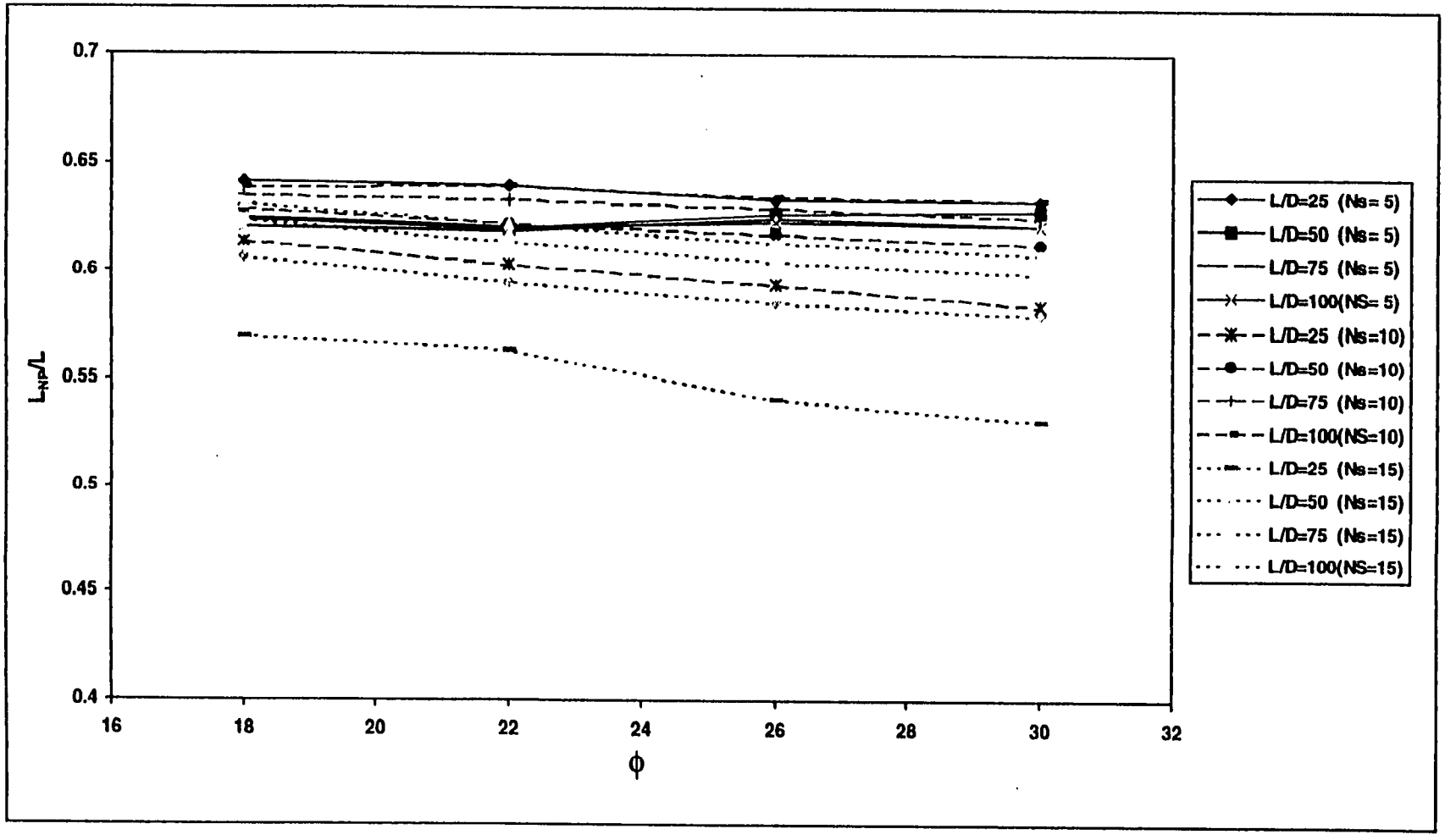

Figure (4-4) The effect of the soil shearing resistance, ϕ, on the location of the neutral plane for FS = 4

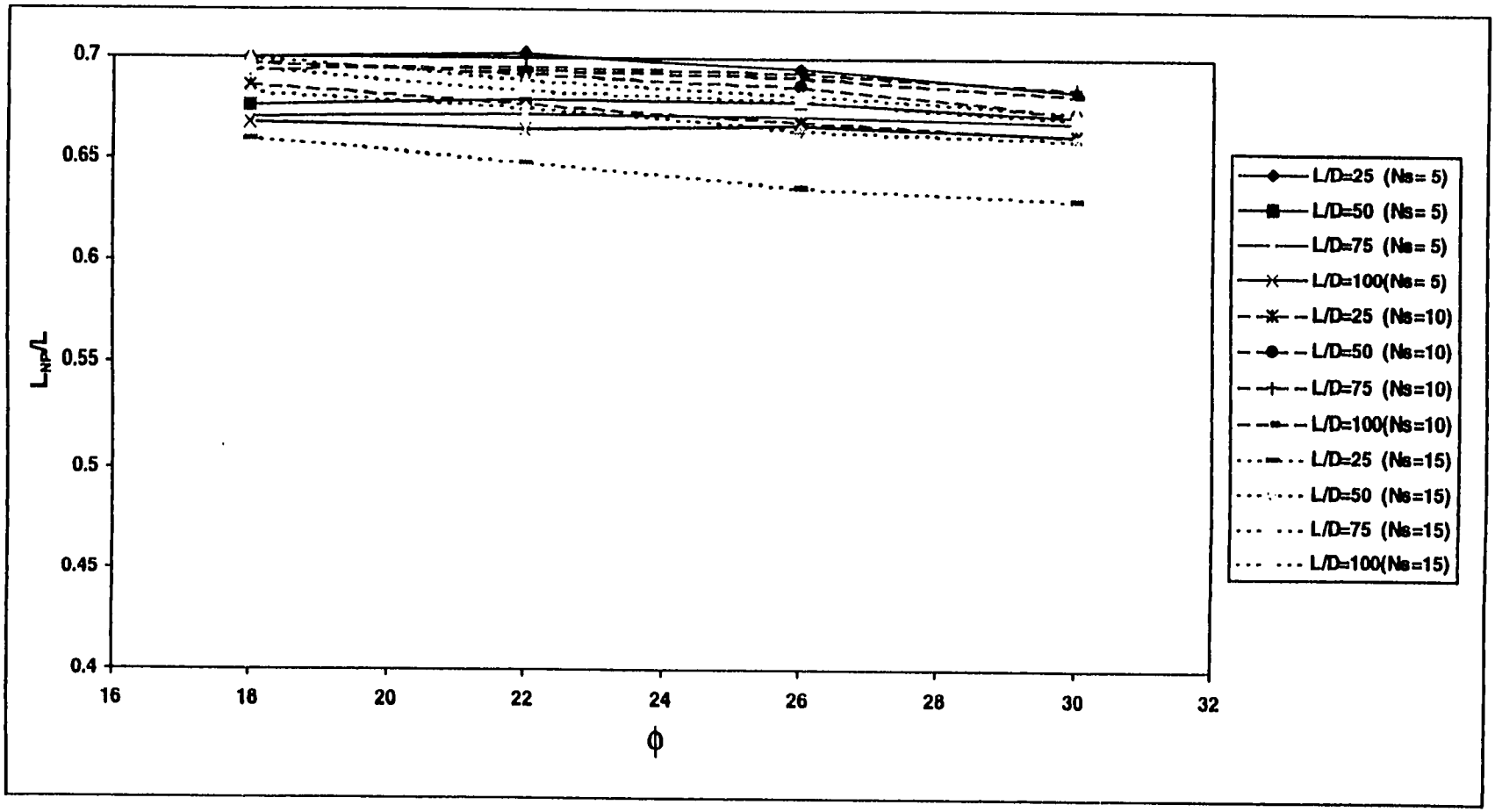

Figure (4-5) The effect of the soil shearing resistance, ϕ, on the location of the neutral plane, for FS = ∞ (no axial load)

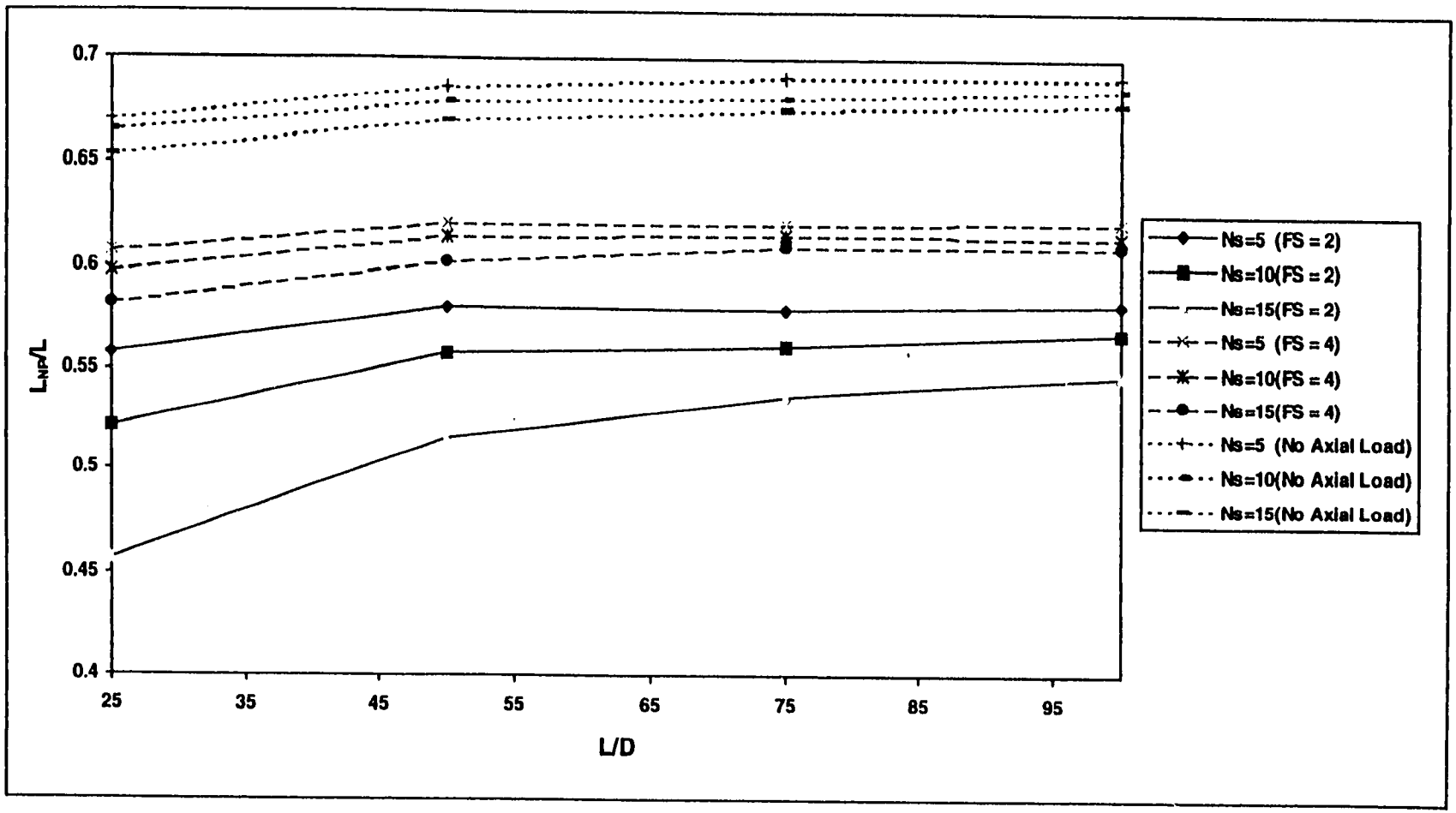

Figure (4-6) The effect of the pile length to the pile diameter ratio, L/D, on the location of the neutral plane

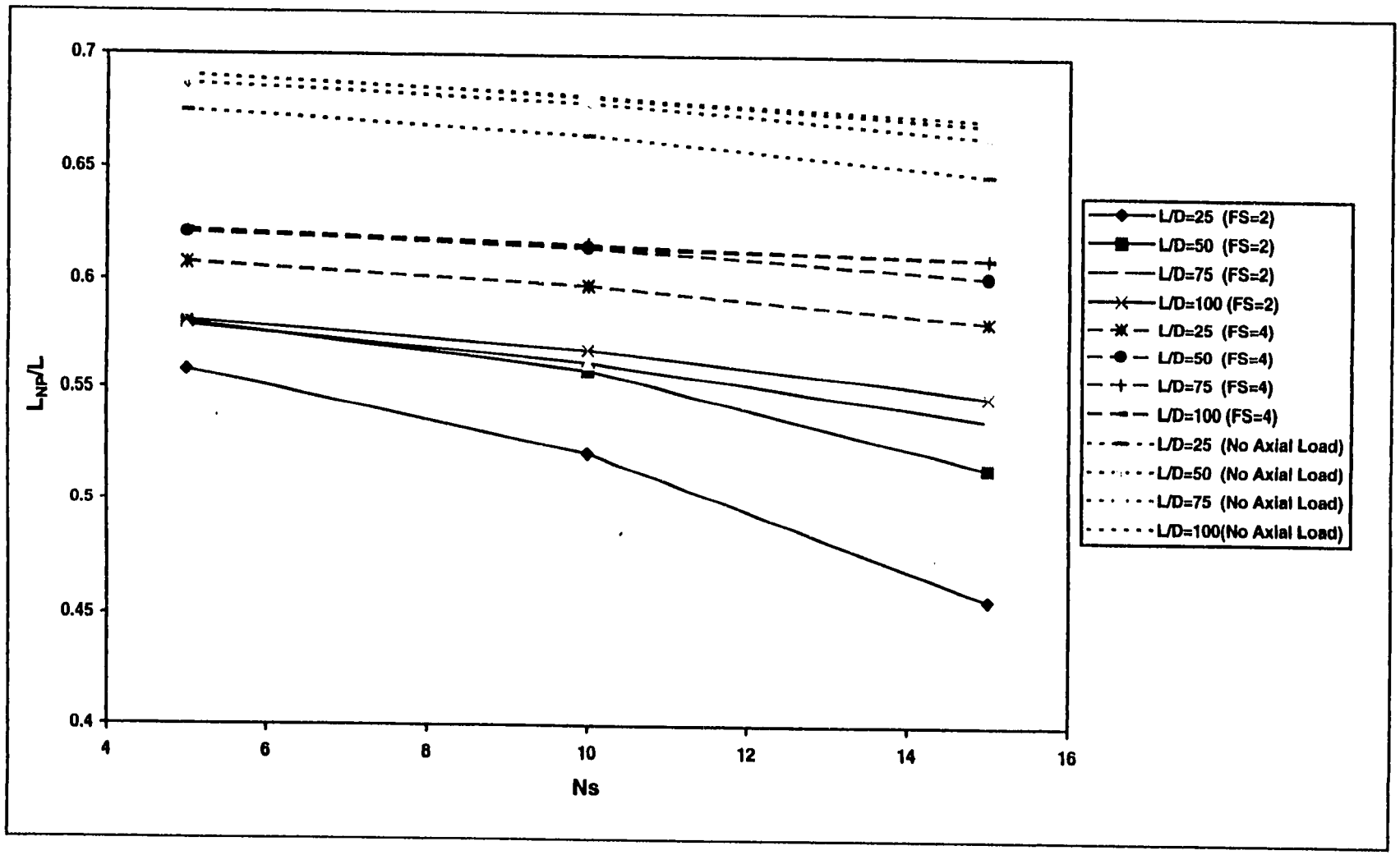

Figure (4-7) The effect of surcharge pressure factor, Ns, on the location of the neutral plane

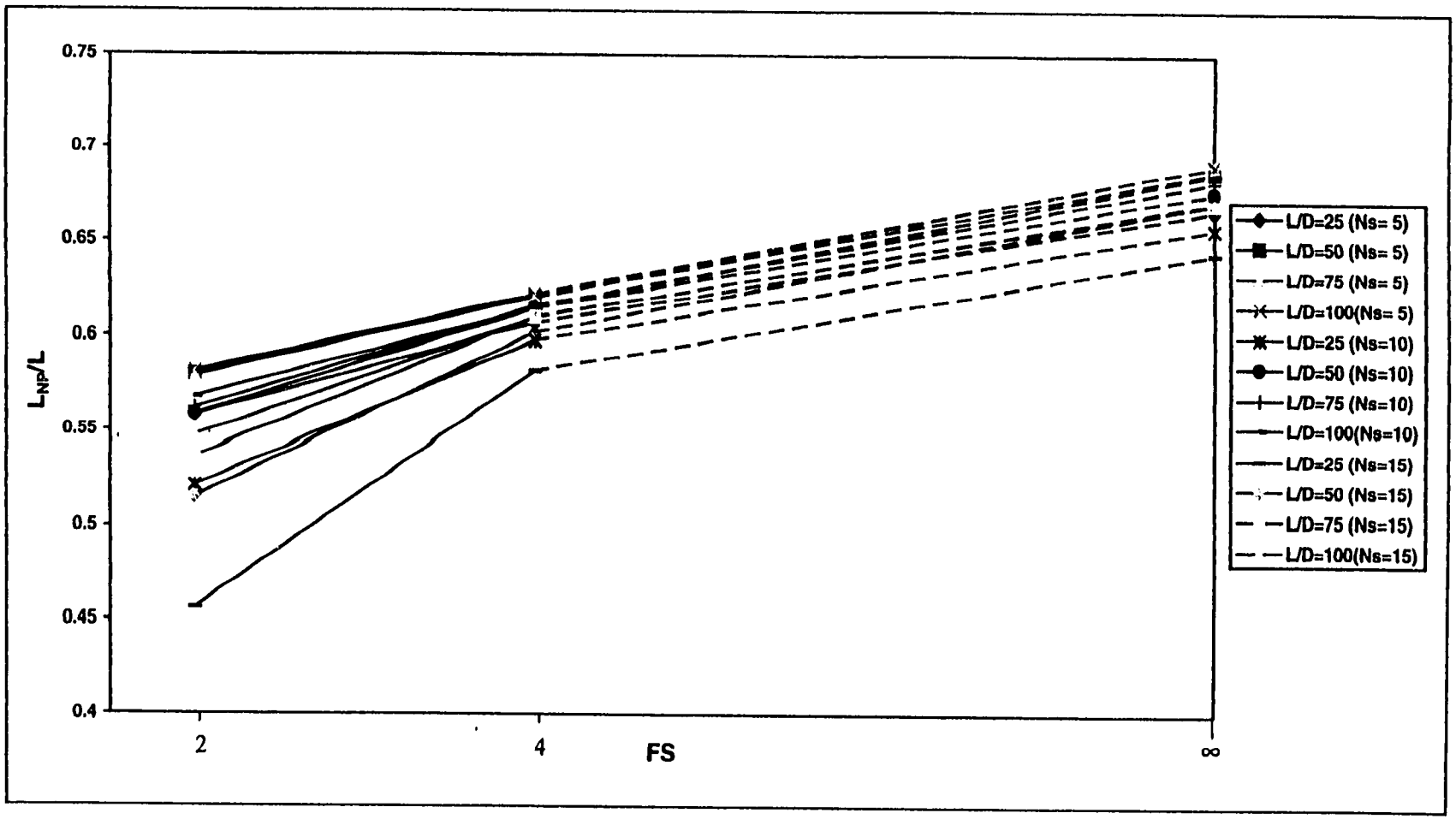

Figure (4-8) The effect of factor of safety, FS, on the location of neutral plane

4.5.5 Discussion

Based on the above parametric study, it can be reported that the neutral plane is greatly affected by the axial load applied on the pile head, the surcharge pressure on the surrounding area of the pile, and the length of pile.

It is of interest to note that the neutral plane vary with the loading condition on the pile. This means that, for a given surcharge pressure, an increase of the axial load will shift the neutral plane upward. Accordingly, the shaft resistance will increase, and thereby the downdrag load will decrease. In contrast, an increase of surcharge pressure will increase the downdrag load, by shifting the neutral plane downward, and decrease the shaft resistance.

The pile length has its effect on the neutral plane with a conjunction of the loading condition. Thus, for a given axial load, the neutral plane moves downward with the increase of the pile length and surcharge pressure. On the other hand, for a given surcharge pressure, the neutral plane moves upward with an increase in axial load and decrease in pile length. It should be noted that most of the length of pile effect is preserved in the range of $L/D < 50$. Furthermore, the effect of the loading condition on the effect of a long pile on neutral plane reduces for the ranges of $Ns > 10$ and $FS > 4$.

To demonstrate the effect of pile length, consider two piles, of 15 m. and 30 m. in length, are embedded in saturated clay. The clay has an effective unit weight of 8 kN/m^3 and $\beta = 0.27$. Both piles are subjected to axial load, $P_a = 820$ kN, and surcharge pressure. $S = 24$ kN/m^2.

For the 15 m. pile, the neutral plane will be located at 8.78m. below the ground surface. Hence, the downdrag load and the shaft resistance are determined to be equal to, $F_n = 264$

kN and Q_s = 155 kN respectively, and the ratio of downdrag load to shaft resistance is equal to, $F_n/Q_s = 1.7$.

Similarly, for the 30 m. pile, the neutral plane will be located at 18.56 m. below the ground surface. Hence, the downdrag load and the shaft resistance are determined to be equal to, F_n = 928 kN and Q_s = 405 kN respectively, and the ratio of downdrag load to shaft resistance is equal to, $F_n/Q_s = 2.3$.

This example shows that the longer pile has a downdrag load equal to 2.3 times its shaft resistance, whereas the shorter one has a downdrag load equal to 1.7 times its shaft resistance, although both piles are subjected to the same loading conditions.

Therefore, it could be concluded that the location of neutral plane can be manipulated by the level of axial load, the intensity of the surcharge pressure, and the magnitude of L/D. As an example, consider a structure founded on piles that can tolerate settlement, then the piles should be designed with a low factor of safety and short embedded length as possible. The low factor of safety ensures that the pile will be subjected to little negative skin friction while settling with the consolidating soil. Whereas, the short length of pile ensures that the pile tip will penetrate the bearing layer to reduce the negative skin friction. On the other hand, if the structure can not tolerate any settlement, the pile should be designed with a high factor of safety and long pile length. In such cases, the downdrag load might be too high to be resisted by the pile, so bitumen coating is needed to relieve the pile from negative skin friction. An advantage of knowing the depth of neutral plane is to locate at what depth the pile should be coated.

4.6 THE DESIGN APPROACH

4.6.1 The design formula

Based on the above discussion in section 4.5.5, a design formula can be developed to predict the allowable bearing capacity of a pile subjected to a given settlement. This can be achieved by considering a floating pile being subjected to negative skin friction, as shown in Figure (4-9). The negative skin friction and positive skin friction are assumed to be fully mobilized. It is further assumed that the skin friction coefficient, β, is equal for both, the negative skin friction and the positive skin friction. To avoid any singularities, it is assumed that there is a discontinuity in the skin friction distribution at the neutral plane. Thus, the downdrag load, F_n, at depth z can be expressed as

$$F_n = \int_0^{L_{NP}} \beta(\pi D z)(\gamma' z + S)\,dz \qquad \ldots\ldots \text{(4.1)}$$

where, $\beta = K_s \tan(\delta)$, usually varies between 0.2-0.3 for clay deposits

K_s = the lateral earth pressure coefficient

δ = the soil-pile interface friction angle

γ' = the submerged unit weight of soil

D = the pile diameter,

L_{NP}= the neutral depth,

S = the surcharge loading

Similarly, the pile shaft resistance, Q_s, at depth $z>L_{NP}$ is equal to

$$Q_s = \int_{L_{NP}}^{L} \beta(\pi D z)(\gamma' z + S)\,dz \qquad \ldots\ldots \text{(4.2)}$$

In Figure (4-9), the extended dashed line in the negative side represents the extreme case of an end-bearing pile (i.e. no movement at the pile tip), in which the negative skin friction is exerted all over the pile shaft. Therefore, to account for settlement effect on the allowable bearing capacity, the downdrag load is better expressed as a ratio of the extreme end-bearing one. Hence,

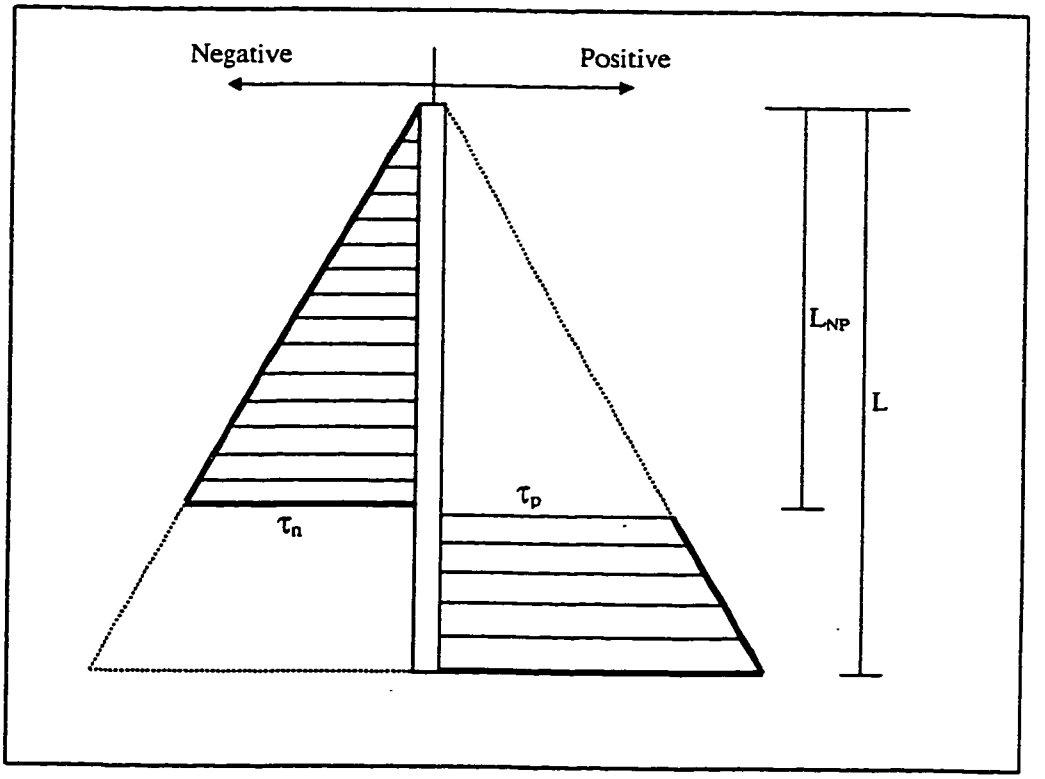

Figure (4-9) Distribution of positive and negative skin friction

$$F_n = R_N F_n^m \qquad \ldots\ldots \text{(4.3)}$$

where,
$$F_n^m = \int_0^L \beta(\pi D z)(\gamma' z + S)\,dz \qquad \ldots\ldots \text{(4.4)}$$

and
$$R_N = \frac{F_n}{F_n^m} = \left(\frac{L_{NP}}{L}\right)^2 \qquad \ldots\ldots \text{(4.5)}$$

It worth mentioning here that the pile cannot fail in the sense of plunging due to the downdrag load F_n. At failure due to bearing capacity, the pile will abruptly penetrate the soil, because of which the negative skin friction will be eliminated. Thus, F_n will not be included in the determination of the allowable bearing capacity of the pile, P_a, expressed by the following:

$$P_a = \frac{Q_t + Q_s}{FS} \qquad \ldots\ldots (4.6)$$

where, Q_t = the ultimate tip resistance of the pile

Q_s = the ultimate shaft resistance acting bellow the neutral plane

FS = the factor of safety

Equation (4.6) dose not account for any settlement restrictions, it only determines the allowable due to bearing capacity perspective. However, the ultimate shaft resistance, Q_s, can also be introduced in terms of the maximum ultimate shaft resistance, Q_s^m, and the downdrag load, F_n, by the following:

$$Q_s = Q_s^m - F_n \qquad \ldots\ldots (4.7)$$

where, $$Q_s^m = \int_0^L \beta(\pi D z)(\gamma' z + S)\,dz \qquad \ldots\ldots (4.8)$$

Hence, by substituting for equation (4.7), equation (4.6)becomes:

$$P_a = \frac{Q_t + Q_s^m}{FS} - R_N F_n^m \qquad \ldots\ldots (4.9)$$

The downdrag load is excluded from being divided by the factor of safety, FS, to ensure the safety side in determining the allowable bearing capacity, P_a. It should be pointed out herein that equation (4.9) is a generalized formula that is capable of estimating the

allowable load of piles resting on different bearing strata, and for different settlement conditions. Furthermore, it can also be used in situation where the pile is needed to be coated with bitumen to reduce the pile settlement. In this case, the reduction factor, R_N, is modified to incorporate the effect of coating expressed as:

$$R_N = \frac{\beta_c}{\beta}\left(\frac{L_{NP}}{L}\right)^2 \qquad \ldots\ldots \textbf{(4.10)}$$

where, β_c = is the Beta-coefficient for bitumen coating conditions, which usually varies between 0.01 to 0.05 (Vesic, 1977)

It has been reported in literature that bitumen coating of as thin as 1.5 mm. is sufficient enough to eliminate nearly all negative skin friction (Walker and Darvall, 1973). This is true if proper caution was taken to ensure that the coating is not stripped off during installation. Two charts are provided in Figures (4-10) and (4-11) to determine R_N for uncoated and coated piles respectively. These charts are limited to floating piles only. The curves provided for coated piles are determined by considering $\beta_c = 0.05$ and $\beta = 0.25$.

4.7.2 Design procedure

The following examples illustrate the design procedure in determining the allowable bearing capacity of a single pile by using the suggested formula and charts.

Consider a floating pile of 15 m. in length and 0.3 m. in diameter embedded in saturated clay subjected to a surcharge loading, S = 10 kN/m^2. Knowing that the soil effective unit weight, $\gamma' = 8$ kN/m^3 and $\beta = 0.25$, for both positive and negative skin friction, and $\beta_c = 0.05$ in case of bitumen or bentonite coating. Determine the allowable

bearing capacity, (a) using FS = 2, (b) using FS = 4 for settlement considerations, and whether a bitumen coating is needed?

To solve this problem, the maximum shaft resistance, Q_s^m, the maximum downdrag load, F_n^m, and the tip resistance, Q_t, must first be determined. Using equations (4.4) and (4.8), then $F_n^m = 247$ KN and $Q_s^m = 247$ KN

For the determination of Q_t, the following relationship can be used

$$Q_t = N_t (\gamma L + S) A_t$$

where, N_t = tip bearing capacity coefficient, which is assumed to be 3.

A_t = the tip area of the pile

Then, $Q_t = 28$ KN

The second step in this problem is to determine the reduction number, R_N. Since, FS = 2, L/D = 50, and Ns = (γL/S) = 12 are given, then from Figure (4-10), $R_N = 0.27$.

Thus the allowable bearing capacity is equal to:

$$P_a = \frac{247 + 28}{2} - 0.27(247) = 70.8 \text{ KN}$$

In case of FS = 4, from Figure (4-10), $R_N = 0.36$, then the allowable bearing capacity is equal to:

$$P_a = \frac{247 + 28}{4} - 0.36(247) = -20.2 \text{ KN}$$

the result of Pa = -20.2 implies that the pile requires a pull-up force equal to -20.2 to hold the pile in position. Thus bitumen coating is necessary for settlement and bearing capacity considerations. The bitumen should be coated in the pile upper portion starting from the

pile head, and extended till the neutral plane. Because of coating $R_N = 0.075$, from Figure (4-11), and hence, the allowable bearing capacity will be equal to:

$$P_a = \frac{247 + 28}{4} - 0.075(247) = 50.2 \text{ KN}$$

It can be noticed from this example the importance of the location of the neutral plane in estimating the allowable bearing capacity and the extent of the coating area. Furthermore, the role and influence of the factor of safety on both the bearing capacity and the neutral plane depth.

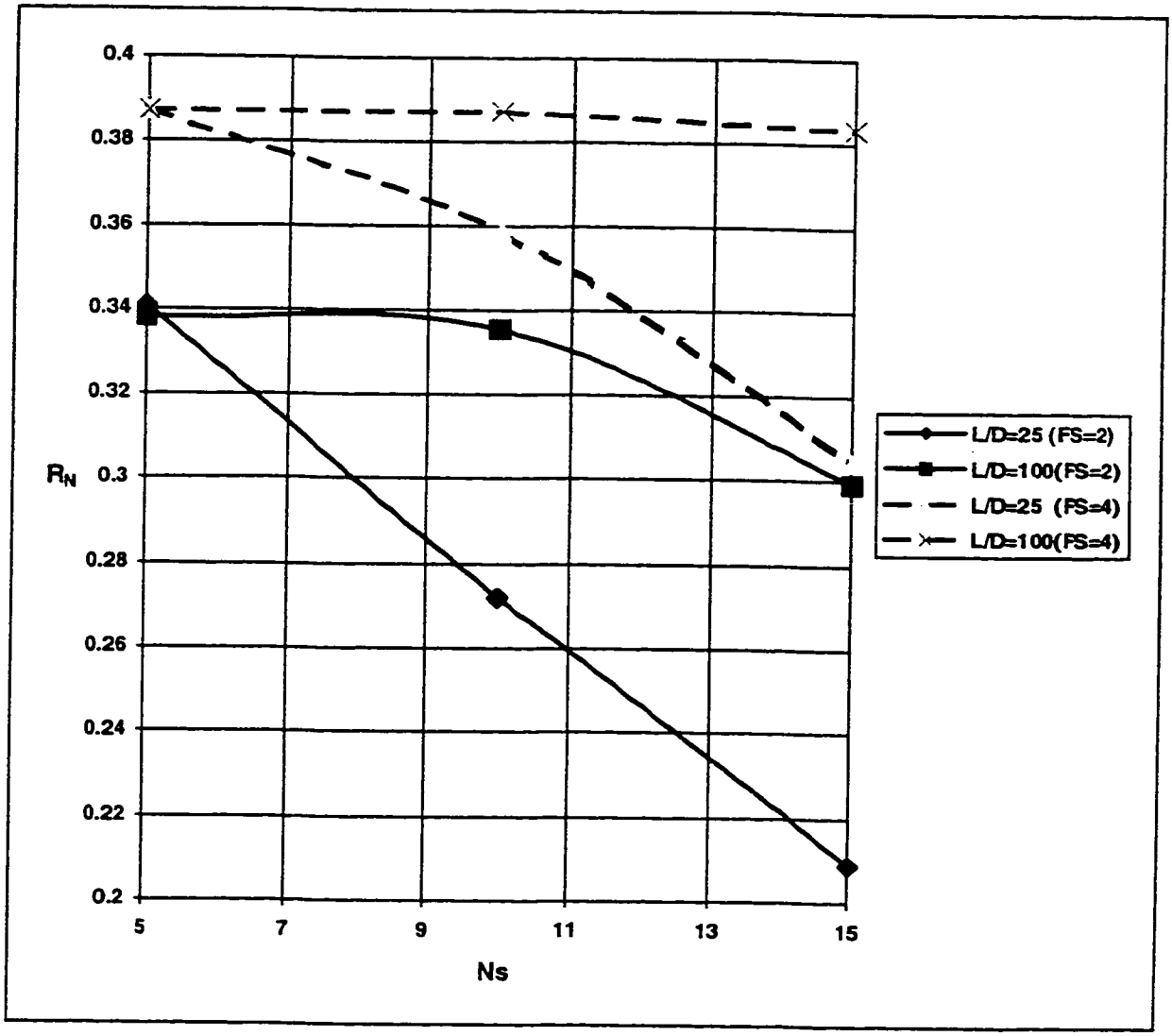

Figure (4-10) The values of the reduction number, R_N, for uncoated piles

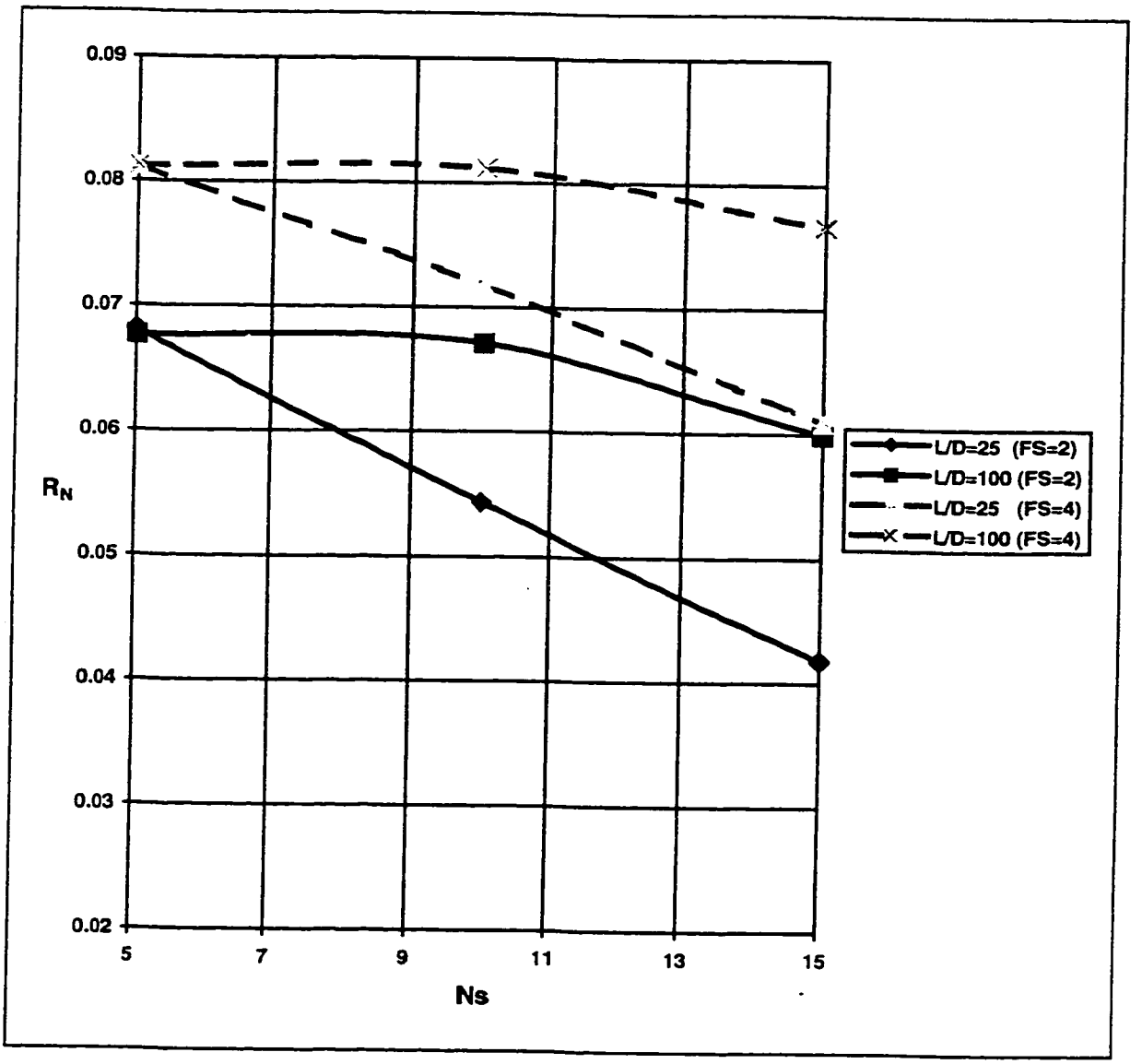

Figure (4-11) The values of the reduction number, R_N, for coated piles

CHAPTER 5
CONCLUSION AND RECOMMENDATIONS

5.1 CONCLUSION

A numerical model was developed and used to determine the location of the neutral plane of a single pile subjected to both direct and indirect loading and embedded in clay. The following can be concluded:

1. The finite element technique in conjunction with an elastic perfectly plastic model (with a yield function defined by the Mohr-Coulomb equation) have proved to be an acceptable numerical model to analyze the negative skin friction on piles.
2. The location of neutral plane is insensitive to the duration of the consolidation process.
3. The soil elastic parameters, E_s and ν_s, have shown no influence on the location of neutral plane.
4. Based on the parametric study the following have been observed:
   (a) The angle of shearing resistance, ϕ, has no considerable effect on the location of neutral plane,
   (b) The depth of neutral plane slightly increases due to the increase of the pile slenderness ratio, L/D. This increase, however, can be ignored for L/D > 50.
   (c) The depth of neutral plane increases with increase of the indirect loading (due to surcharge pressure), especially for short piles.
   (d) The depth of neutral plane increases considerably due to the increase of factor of safety, FS, until FS = 4, after which the increase drops significantly.

5. A design formula together with design charts are presented to predict the allowable bearing capacity for coated and uncoated single piles.

5.2 RECOMENDATIONS FOR FURTHER RESEARCH

1. The present study should be extended to investigate the other causes of consolidation, such as, fluctuation of the groundwater table and the pile installation in sensitive clay.
2. The present investigation should be extended to examine the effect of the compressibility of the bearing layer.
3. The effect of the location and extension of the surcharge pressure on the depth of the neutral plane.
4. Further numerical studies are required to examine the effect of negative skin friction on battered piles.
5. The effect of the direct load variation with time on the location of neutral plane.

REFERENCES

1. **Auvinet, G. and Hanell, J. (1981)**, " Negative Skin Friction on Piles in Mexico Clay," Proc. 10th Conf. S.M. & F.E., Stockholm, Sweden, Vol. 2, pp. 65-74.
2. **Bozozuk, M. (1970)**, " Field Observation of Negative Skin Friction Loads on Long Piles in Marine Clay," Proc. Conf. on Design and installation of Pile Foundation and Cellular Structures, Lehigh University, pp. 273-280.
3. **Bozozuk, M. (1972)**, " Downdrag Measurements on a 160-Ft Floating Pipe Test Pile in Marine Clay," Can. Geotech. J., Vol. 9, No. 2, pp. 127-136.
4. **Brand, E. W. and Luangdilok, N. (1975)**, " A Long-term Foundation Failure Caused by Dragdown on Piles," 4th Southeast Asian Conference on Soil Engineering, Kuala Lumpur, Malaysia, pp. 4.15 - 4.24.
5. **Brito, A. M. (1995)**, "Crisp95 user and Programmer's Guide," Engineering Department, Cambridge University, UK.
6. **Clayton, C. R. I. and Milititsky, J. (1986)** *Earth Pressure and Earth-retaining Structures.* Surry University Press. Glasgow. UK.
7. **Clement, F. M. Jr. (1984)**, "Downdrag, Negative Skin Friction, and Bitumen Coating on Prestressed Concrete Piles," Ph.D. Thesis submitted to the University of Tulane.
8. **Desai, C. S., Zaman, M. M., Lightner, J. G., and Siriwardene, H. J. (1984)**, "Then-layer Element for Interfaces and Joints," Int. J. Num. & Anal. Meth. Geom., Vol. 8, pp. 19-43.

9. **Esmail, H. (1996)**, "Neutral Plane of Single Piles in Clay Subjected to Surcharge Loading," M.A.Sc. Thesis, Concordia University, Montreal, Quebec, Canada.

10. **Feda, J. (1976)**, " Skin Friction of Piles," Proc. 6th European Conf. S.M. & F.E., Vol. 1.2, pp. 423-428.

11. **Fellenius, B. H. (1972)**, " Downdrag on Piles in Clay due to Negative Skin Friction," Can. Geotech. J., Vol. 9, No. 4, pp. 323-337.

12. **Fellenius, B. H. (1989)**, " Unified Design of Piles and Pile Groups," Transportation Research Record, No. 1169, pp. 75-82.

13. **Fleming, W. G. K., Weltman, A. J., Randolph, M. F., and Elson, W, K. (1985)**, *Piling Engineering*. 1st edition, John Wiley & Sons Inc., New York.

14. **Garlanger, J. E. (1974)**, " Measurement of Pile Downdrag beneath a Bridge Abutment," Highway Research Board, Trans. Res. Record No. 517, pp. 61-69.

15. **Janbu, N. (1976)**, " Static Bearing Capacity of Friction Piles," Proc. 6th European Conf. S.M. & F.E., Vol. 1.2, pp. 479-488.

16. **Lee, C. Y. (1993)**, " Pile Groups Under Negative Skin Friction," J. Geotech. Engng. Div., ASCE, Vol. 119, No. 10, pp. 1587-1600.

17. **Leung, C. F., et al (1991)**, " Performance of Precast Driven Piles in Marine Clay," J. Geotech. Engng. Div., ASCE, Vol. 117, No. 4, pp. 637-657.

18. **Lim, C. H., Chow, Y. K., and Karunaratne, G. P. (1993)**, " Negative Skin Friction on Single Piles in a Layered Half-space," Int. J. Num. & Anal. Meth. Geom., Vol. 17, pp. 625-645.

19. **Poorooshasb, H and Bozozuk (1967)**, " Skin Friction on a Single Pile to Bedrock," Proc. 3rd Pan-American Conf. on S.M. & F.E., Caracas, Venezuela, Vol. 1, pp. 613-621.

20. **Poorooshasb, H. B., Alamgir, M., and Miura, N. (1996)**, " Negative Skin Friction on Rigid and Deformable Piles," Computers and Geotechnics, Vol. 18, No. 2, pp. 109-126.

21. **Poulos, H. G. and Mattes, N. S. (1969)**, " The Analysis of Downdrag in End-Bearing Piles," Proc. 6th Int. Conf. S.M. & F.E., Mexico City, Vol. 2, pp. 203-209.

22. **Poulos, H. G. and Davis, E. H. (1972)**, " The Development of Negative Friction With Time in End-Bearing Piles," Aust. Geomechanics Jour., Vol. G2, No. 1, pp. 11-20.

23. **Randolph, M. F. (1977)**, " A Theoretical Study of the Performance of Piles," Ph.D. Thesis, Cambridge University, Cambridge, England.

24. **Randolph, M. F. and Wroth, C. P. (1978)**, " Analysis of Deformation of Vertically Loaded Piles," J. Geotech. Engng. Div., ASCE, Vol. 104, No. GT12, pp. 1465-1488.

25. **Trochanis, A. M., Bielak, J., and Christiano, P. (1988)**, " A Three Dimensional Non-linear Study of Piles Leading to the Development of a Simplified Model," A Technical Report of Research, The National Science Foundation, Carnegie Mellon.

26. **Van Der Veen, C. (1986)**, " A General Formula to Determine the Allowable Pile Bearing Capacity in Case of Negative Friction," International Conference on Deep Foundations, Beijing, China, pp. 2.138-2.147.

27. **Vesic, A. S. (1977)**, " Design of Pile Foundation," National Cooperative Highway Research Program, Synthesis of Highway Practice No. 42, Transportation Research Board, National Research Council, Washington D. C.

28. **Walker, L. K. and Darvall, P. LeP. (1970)**, " Some Aspects of Dragdown on Piles," Proc. 2nd South-East Asian Conf. on Soil Eng., Singapore, pp. 121-137.

29. **Wong, K. S. and Teh, C. I. (1995)**, " Negative Skin Friction on Piles in Layered Soil Deposits," J. Geotech. Engng. Div., ASCE, Vol. 121, No. 6, pp. 457-465.

30. **Zeevaert, L. (1959)**, " Reduction of Point Bearing Capacity of Piles Because of Negative Friction," Proc. 1st Pan-American Conf. on S.M. & F.E., Mexico. Vol. 3, pp. 1145-1152.